TAMPERE UNIVERSITY OF TECHNOLOGY

AYMAN BARAKAT

EVALUATION OF AN EXISTING APPROACH FOR OSCILLATOR POWER OPTIMIZATION

Master of Science Thesis

Examiners: Prof. Olli-Pekka Lunden
and Dr. Tech. Jari Kangas
Examiners and topic approved by
the Faculty Council of the Faculty of
Computing and Electrical Engineering on 8 May 2013.

ABSTRACT

TAMPERE UNIVERSITY OF TECHNOLOGY
Master's Degree Programme in Electrical Engineering
BARAKAT, AYMAN: Evaluation of an Existing Approach for Oscillator Power Optimization
Master of Science Thesis, 41 pages, 31 Appendix pages
June 2013
Major: Radio Frequency Electronics
Examiners: Prof. Olli-Pekka Lunden and Dr. Tech. Jari Kangas
Keywords: RF oscillators, power optimization, negative resistance

Oscillators nowadays are indispensable components in most of electronic devices. Different theories have been developed to design and analyze oscillators. However, due to their nonlinearity and structure complexity, the design of an optimal Radio Frequency (RF) or microwave oscillator is not simple, and is subjected at the end to practical experiments. This thesis evaluates one of the approaches used to optimize the oscillator output power on the basis of maximizing the negative real part of the small-signal output immittance. The main goal is to examine whether the output power can be maximized by maximizing the small-signal negative resistance/conductance or not. And in more general words, we want to check if we are capable to predict or control a large-signal parameter (as output power) by just using a small-signal parameter (as negative resistance or conductance). To reach our goal, a computer aided design tool was used, and also practical experiments were carried out for a BJT Clapp oscillator. The negative real part of output immittance at startup was recorded as a function of variable feedback reactances, and the corresponding output power was also recorded while the load was kept always at its optimal value. This procedure was performed for parallel- and series-load orientations and a range of coupling capacitor ratios.

The study revealed disagreement with this approach that aimed to maximize the output power by maximizing the small-signal negative resistance/conductance. The maximum output power was not delivered by maximizing the output small-signal negative resistance or conductance, but it was delivered at a less negative resistance/conductance value. The results suggest not to rely on this approach for optimizing the oscillator output power. Moreover, we recommend for further analytic studies to explore the behaviour of the negative resistance or conductance in terms of the oscillation amplitude, especially when reaching the steady-state point.

PREFACE

This thesis was written for the Department of Electronics and Communication Engineering at Tampere University of Technology (TUT). The thesis topic is related to my Major study in RF Electronics. The practical experiments were carried out in TUT's RF laboratory. I would like to thank Prof. Olli-Pekka, as a supervisor and an examiner, for providing me this topic, and for his valuable guidance, support and feedback during all work stages. Due to his generous treatment and kind patience, He has turned the thesis from a heavy burden into an exciting work. I would like to thank my examiner, Dr. Tech. Jari Kangas, for his advices and feedback that enhanced the thesis quality. I am so grateful to Tampere University of Technology for providing a perfect environment for studying, and for giving me a good chance to obtain my master degree. Finally, I would like to give special thanks to my friends here in Tampere who supported me during my stay in Finland, and to my family in Egypt for their love, support and encouragement.

Tampere, May 17, 2013.

Ayman Barakat

CONTENTS

LIST OF FIGURES

LIST OF TABLES

LIST OF SYMBOLS AND ABBREVIATIONS

AC	Alternating current
BJT	Bipolar junction transistor
DC	Direct current
FET	Field-effect transistor
GaAs	Gallium Arsenide
IMPATT	Impact ionization avalanche transit-time
RF	Radio frequency

1. INTRODUCTION

RF oscillators are one of the main building blocks used in RF electronic systems. They simply convert DC into an RF alternating signal, and often consist of an amplifier network connected to a positive feedback network. And, under a certain criterion, this configuration can produce oscillations, having a constant amplitude and frequency, and they can be considered stable or "steady-state" oscillations. A long list of applications which rely on the RF signal generated by oscillators can be mentioned here. But mainly, oscillators are used wherever an RF signal is needed such as in modulation and demodulation processes in RF communication transceivers. Also, they are acting as precise clocks in computers, radars and various navigation systems [14].

One of the commonly used oscillators is the Clapp oscillator, which belongs to the family of LC-oscillators. It has a similar construction as the Colpitts oscillator, with an extra tuning (resonator) capacitance added in series with the resonator inductance to separately tune for the desired oscillation frequency, and provides higher frequency stability compared to Colpitts [1]. Thus Clapp oscillator can work as a Variable Frequency Oscillator (VFO) or a Voltage Controlled Oscillator (VCO) if the resonator capacitance is variable and controlled by DC voltage as in varactor diodes.

Oscillators operate in the nonlinear region of the current-voltage characteristic curve of their active device. Moreover, the impedance seen from oscillator networks are finite. For these reasons, analyzing oscillator using *transfer function* definitions is not the best way. Two significant theories are developed to analyze oscillators. The feedback oscillator theory is based on considering its circuit as a loop of two networks, amplifier and feedback, with a unity gain and zero phase shift. Whereas the one port negative resistance/conductance theory divides the circuit into two parts, active and passive, where the active part is a one port network having a negative output resistance/conductance and containing the active device, while the passive part is the load or the resonator. In practice, a guaranteed oscillation, at the desired frequency and sufficient output power, depends also on trials during practical laboratory experiments because these methods are still insufficient to produce complete design basis.

Considerable amounts of research have aimed to study and optimize the oscillator output power as in [7; 2; 8]. For instance, Maeda has designed a GaAs Schottky-gate FET oscillator based on a certain approach for optimizing the output power [2]. This approach selects the optimum feedback reactances, which give the maximum absolute value of the

oscillator output negative resistance, and supposedly, ensures oscillation with maximum output power. Likewise, Grebennikov [8], has followed the same approach while developing a general analytic expression for the optimum real and imaginary parts of the output immittance, which produce the maximum output power. This approach uses the small-signal parameters of the oscillator to predict the behaviour of a large-signal parameter as output power. Accordingly, one may question if that approach is really leading to find the highest possible output power, and why should the maximum output power be related to the maximum small-signal negative output resistance or conductance. Fortunately, there are many computer aided design tools that enable us to test both small-signall and large-signal behaviour of RF circuits. Thus, one can test Maeda's and Grebennikov's approach.

This thesis examines the validity of the above approach for optimizing the oscillator output power, and assesses for a design example the relation between the negative real part of the output immittance and the output power of an RF oscillator. The study is based on the negative resistance/conductance concepts, and uses computer-aided methods to analyze a BJT Clapp oscillator connected to parallel or series load. In addition, practical experiments are performed to confirm the main outcomes. The thesis begins with a theoretical background about oscillators and existing approaches for their power optimization. Then, it introduces the evidences that oppose the approach - under study - through computer simulations and laboratory measurements. Finally, a conclusion is given to summarize the whole thesis. The thesis enriches the studies meant to optimize the oscillator power from the negative resistance/conductance concept perspective.

2. THEORETICAL BACKGROUND

An oscillator converts DC into a periodic signal at a certain frequency without any aid of external input AC signals. This periodic signal usually has a sinusoidal shape in RF oscillators [3, p. 650]. In the next sections, we review the basic theories of oscillators such as feedback and negative resistance theories. Next, we present some approaches for optimizing the output power.

2.1 Feedback theory

To understand the main idea behind oscillator's design, we assume an amplifier with a voltage gain $A(\omega)$, connected to a feedback network with a transfer function $B(\omega)$, as shown in Figure 2.1. By the mentioned configuration, the relation between input and

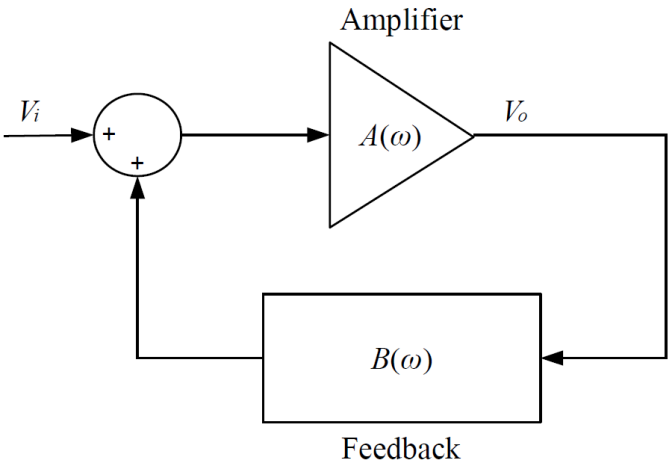

Figure 2.1: Amplifier with a positive feedback network.

output voltage is [4, p. 384–385], [5, p. 540]:

$$V_o = \frac{A(\omega)}{1 - A(\omega)B(\omega)} V_i. \tag{2.1}$$

From equation (2.1), the only way to maintain a non-zero output voltage without applying an input voltage is to set the denominator of equation (2.1) to zero, producing the steady-state oscillation condition or the so-called *Barkhausen criterion* [4, p. 385–386], [5, p. 540]:

$$A(\omega)B(\omega) = 1. \tag{2.2}$$

The above condition means that to obtain steady-state oscillations at a certain frequency, the loop gain $A(\omega)B(\omega)$ must equal unity. Since both of amplifier and feedback transfer functions are complex, then the above condition can be split into two inseparable conditions:

$$|A(\omega)B(\omega)| = 1, \tag{2.3}$$

$$\Phi_A + \Phi_B = n \times 360\,^\circ, \tag{2.4}$$

where Φ_A and Φ_B are the amplifier and feedback phase shifts, respectively, and n is an integer equal to 0, 1, 2, ... Equation (2.3) represents the gain condition, which implies that the loop gain magnitude must equal to unity, to ensure a stable or constant amplitude oscillation. While equation (2.4) represents the oscillation frequency condition, which tells that the total loop gain phase shift must equal to zero or multiples of $360\,^\circ$, to ensure an oscillation at certain frequency. So if both conditions are met, a steady-state oscillation will be achieved with constant amplitude at a certain frequency.

The non-inverting amplifiers have a real voltage gain with constant magnitude and zero phase shift. Whereas the inverting amplifiers are the same but they have $180\,^\circ$ phase shift. So if we consider an ideal case of either noninverting or inverting amplifier, then both real and imaginary parts of Barkhausen criterion can be written as [4, p. 385–386]:

$$A_o = \frac{1}{B_r(\omega)}, \tag{2.5}$$

$$B_i(\omega) = 0, \tag{2.6}$$

where A_o is the amplifier constant gain, $B_r(\omega)$ and $B_i(\omega)$ are the real and imaginary parts of the feedback transfer function, respectively. Equations (2.5) and (2.6) show that for a non-inverting or inverting amplifier, the feedback transfer function must be real and in-phase with the amplifier gain to maintain Barkhausen criterion. Barkhausen criterion should be satisfied at the steady-state condition. But at startup, the loop gain magnitude should be greater than unity to build up the oscillation amplitude. Therefore, the gain condition at startup is [5, p. 541]:

$$|A(\omega)B(\omega)| > 1. \tag{2.7}$$

Practically, the input signal at startup should not be zero, but it is enough to start oscillation by a very low input signal such as noise or switching transients. This input signal grows due to the startup condition producing an unstable oscillation at the beginning, until the amplifier transconductance saturates to achieve unity loop gain magnitude. At this moment, the oscillator reaches steady-state oscillation with a significant output amplitude. [6, p. 30] Figure 2.3 shows the output voltage waveform in time domain from startup to steady-state for a simulated Clapp oscillator. As shown in Figure 2.2, the oscillator's am-

plifier consisted of a BJT with its biasing circuit, and connected to 50-Ω load through a matched network ($L_e = 200$ nH and $C_e = 15$ pF). While the feedback network consisted of a series resonator and coupling capacitors. The series resonator consisted of a 370-nH resonator inductor and 12-pF resonator capacitor, and the coupling capacitances C_1 and C_2 were 18 and 10 pF, respectively. From this figure we notice that the startup time is about 150 nsec, and it may vary depending on the resonator quality factor, loop gain and oscillation frequency [6, p. 106–108].

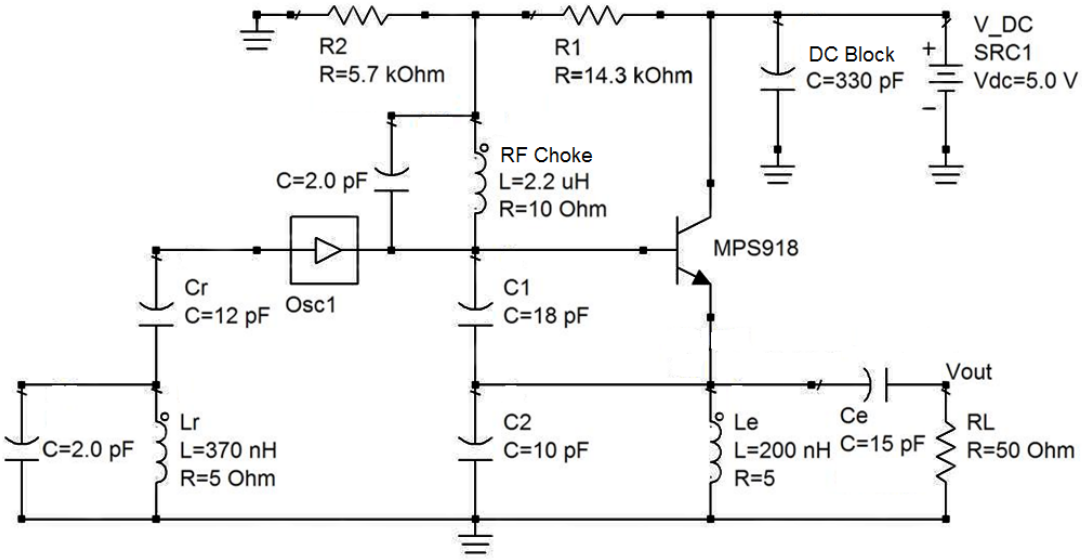

Figure 2.2: Schematic circuit of 100 MHz Clapp oscillator. The biasing circuit consists of 5-V DC source, and two biasing resistors, R_1 and R_2, connected to 2.2-μH RF choke. In some later figures, the biasing circuit is omitted for simplicity.

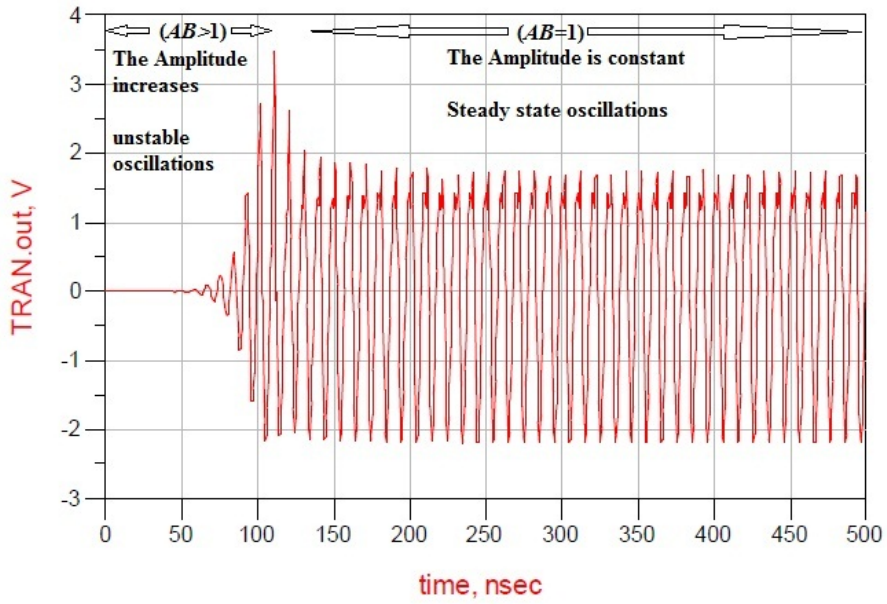

Figure 2.3: A 100 MHz Clapp oscillator output voltage in time domain. The schematic is given in Figure 2.2.

Usually, the transfer function definition is the open circuit output voltage divided by the input voltage produced from a voltage source with zero internal resistence. Conversely, both amplifier and feedback transfer functions see a finite input impedance and nonzero output impedance. Therefore, using the feedback theory, in designing RF oscillators, may lead to approximating the impedance values, and consequently, producing inaccurate results. The next section presents another theory that avoids the finite impedance problem.

2.2 Negative resistance theory

In general, the one port negative resistance oscillator circuit consists of two parts. The first part is the active part, which is formed by connecting the active device to either the load or the resonator. This part is a one port network and has a negative resistance as it produces power. The second part is the passive load or resonator which has a positive resistance as it consumes power. Figure 2.4 shows an example of a negative resistance analysis on a Clapp oscillator where the load is the passive part.

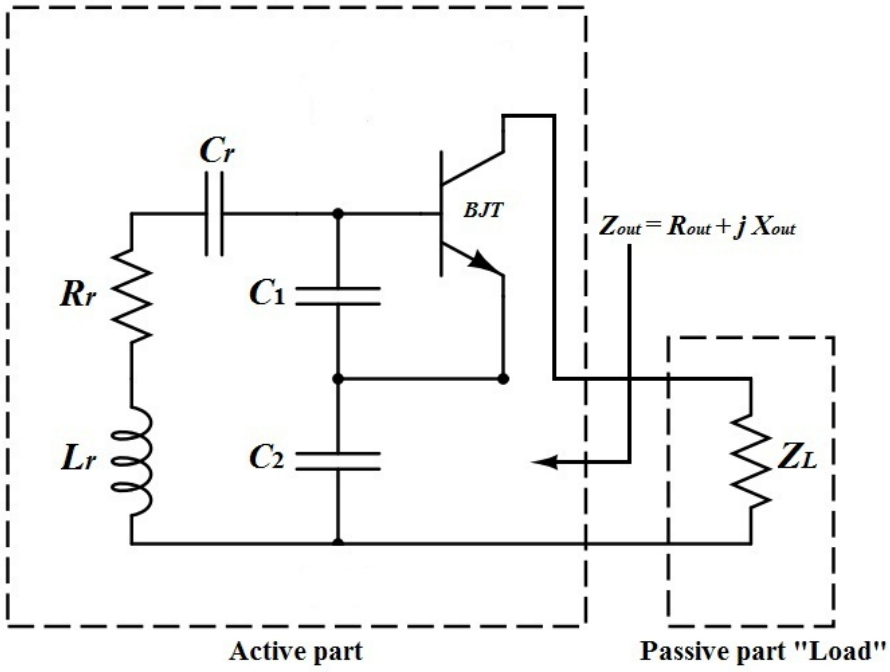

Figure 2.4: Clapp oscillator schematic analyzed by the negative resistance theory. The two port active device is connected to a feedback network. R_r is the resonator equivalent series resistance. Biasing circuit is omitted.

The circuit oscillates when the net impedance is equal to zero at the steady-state frequency. Thus a current will circulate through the circuit without diminishing even if no input AC source connected. [15, p 562.] Figure 2.5 shows the oscillator equivalent circuit after simplification. The steady-state oscillation condition can be written as [4, p. 389]:

$$Z_{out}(A_o, \omega_o) + Z_L(\omega_o) = 0, \tag{2.8}$$

where A_o is the steady state current amplitude, and ω_o is the steady state oscillation

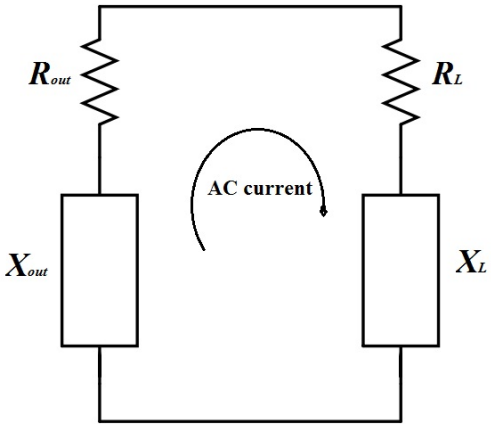

Figure 2.5: A simplified oscillator equivalent circuit based on the negative resistance analysis.

frequency. The output and load impedances can be expressed as follows:

$$Z_{out}(A_o, \omega_o) = R_{out}(A_o, \omega_o) + X_{out}(A_o, \omega_o), \tag{2.9}$$

$$Z_L(\omega_o) = R_L(\omega_o) + X_L(\omega_o). \tag{2.10}$$

By substituting (2.9) and (2.10) in equation (2.8), and separating real and imaginary parts, we can write the steady-state oscillation conditions as follows [4, p. 389]:

$$R_{out}(A_o, \omega_o) + R_L(\omega_o) = 0, \tag{2.11}$$

$$X_{out}(A_o, \omega_o) + X_L(\omega_o) = 0. \tag{2.12}$$

Assuming a pure resistive load (i.e, $X_L(\omega_o) = 0$) in the above configuration of the Clapp oscillator shown in Figure 2.4, then equation (2.12) can be written as:

$$X_{out}(A_o, \omega_o) = 0. \tag{2.13}$$

By expressing X_{out} in terms of the feedback elements, the oscillation (resonance) frequency f_o at steady-state can be found as follows [5, p. 571–572]:

$$j(\omega_o L_r - \frac{1}{\omega_o C_r} - \frac{1}{\omega_o C_1} - \frac{1}{\omega_o C_2}) = 0, \tag{2.14}$$

$$f_o = \frac{1}{2\pi}\sqrt{\frac{1}{L_r}(\frac{1}{C_r} + \frac{1}{C_1} + \frac{1}{C_2})}. \tag{2.15}$$

At startup, the net resistance should be negative to build up the oscillation amplitude.

Therefore, oscillation startup condition is as follows [4, p. 389]:

$$|R_{out}(0,\omega)| > R_L(\omega), \tag{2.16}$$

where $R_{out}(0,\omega)$ is the initial output resistance of the active part. Depending on the behaviour of R_{out} as a function of the output current amplitude, and load configuration, oscillator circuits are analyzed by either negative resistance or conductance concept [15, p. 562–573]. Hence for those circuits analyzed by negative conductance concept, the steady state oscillation conditions can be written as [5, p. 393394]:

$$G_{out}(A_o,\omega_o) + G_L(\omega_o) = 0, \tag{2.17}$$

$$B_{out}(A_o,\omega_o) + B_L(\omega_o) = 0, \tag{2.18}$$

and the startup condition is [4, p. 394]:

$$|G_{out}(0,\omega)| > G_L(\omega), \tag{2.19}$$

where G_{out} and G_L are the output and load conductances, respectively, and B_{out} and B_L are the output and load susceptances, respectively. The one port negative resistance/conductance analysis can be applied in a similar manner if the oscillator circuit is divided from the resonator side.

2.3 Existing approaches for output power optimization

In many cases, scientists are interested in knowing how to optimize oscillator's output power by choosing optimum feedback elements and load. In this section, we will review two approaches for optimizing the oscillator output power. The first approach depends on the selection of the load value, while the second approach depends on the selection of the feedback elements' values.

2.3.1 The optimum load approach

This is one of the approaches that aimed to optimize oscillators output power. According to his study on the IMPATT diode oscillator [7], Gewartowski has found that the relation between the IMPATT diode negative conductance magnitude and the output voltage magnitude can be represented approximately by a straight line, as shown in Figure 2.6. And, he used this relation to prove theoretically that the maximum oscillator power is obtained when the diode negative conductance magnitude is one third of its maximum initial (or startup) value at a given biasing conditions. [7.] This approach has been widely used [2; 4, p. 390–394; 3, p. 616].

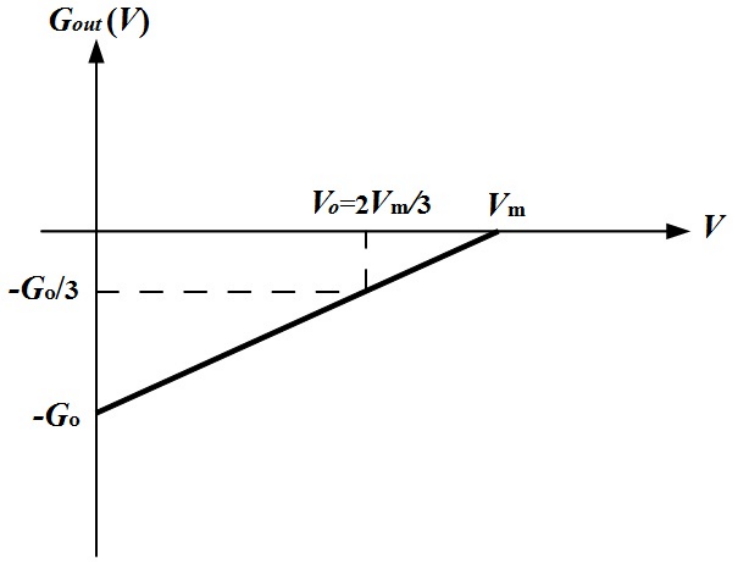

Figure 2.6: Approximated linear relation between the output negative conductance and the output voltage amplitude [7; 4, p. 390]

Generally, from Figure 2.6, the optimum output conductance can be derived as follows [7; 4, p. 390–394]:

$$G_{out}(V) = -G_o(1 - \frac{V}{V_m}), \tag{2.20}$$

where G_o is the absolute initial output conductance, V is the output voltage amplitude, and V_m is the maximum voltage amplitude. By knowing that G_L is equal to $-G_{out}(V)$ at steady state, the output power can be written as:

$$P = \frac{1}{2}V^2 G_L = \frac{1}{2}V^2 G_o(1 - \frac{V}{V_m}). \tag{2.21}$$

Then we find the voltage amplitude that maximizes the output power:

$$\frac{dP}{dV} = \frac{1}{2}G_o(2V - \frac{3V^2}{V_m}) = 0. \tag{2.22}$$

By solving equation (2.22), the optimum voltage amplitude is $V_o = \frac{2}{3}V_m$. By substituting $V = V_o$ in equation (2.20), we deduce the value of G_{out} which maximizes the output power as follows:

$$G_{out}(V_o) = -G_o(1 - \frac{2V_m}{3V_m}) = -\frac{1}{3}G_o. \tag{2.23}$$

From equation (2.17), the optimum load that maximizes the output power should have the following conductance:

$$G_L = -G_{out}(V_o) = \frac{1}{3}G_o. \tag{2.24}$$

Similarly, when the circuit is analyzed by the negative resistance concept, then the

output resistance, as a function of current amplitude, can be optimized as follows:

$$R_{out}(A_o) = -\frac{1}{3}R_o, \tag{2.25}$$

where R_o is the absolute value of the initial output resistance. And the optimum load should have the following resistance:

$$R_L = \frac{1}{3}R_o. \tag{2.26}$$

2.3.2 The maximum negative resistance/conductance approach

Another approach to maximize the output power depends on the design of the feedback elements. Maeda, followed by Grebennikov, has claimed that an optimum combination of the feedback elements, which maximizes the negative real part of the small-signal output immittance, ensures oscillations *with maximum amplitude*, and produces *maximum output power*. In other words, a larger initial negative resistance or conductance leads to a larger output amplitude and higher output power, as shown in Figure 2.7. [2; 8; 9; 10]

For instance, if the resonator and coupling reactances are X_1 and X_2, respectively, then their optimum values X_1^0 and X_2^0 that maximize R_{out} are the solutions of the following equations [8]:

$$\frac{\partial R_{out}}{\partial X_1} = 0, \tag{2.27}$$

$$\frac{\partial R_{out}}{\partial X_2} = 0. \tag{2.28}$$

Hence, the optimum output resistance R_{out}^0 and reactance X_{out}^0 for maximum output power are:

$$R_{out}^0 = R_{out}(X_1^0, X_2^0), \tag{2.29}$$

$$X_{out}^0 = X_{out}(X_1^0, X_2^0). \tag{2.30}$$

After optimizing the output impedance of the active part, we can calculate the optimum load, according to Gewartowski's approach, as follows:

$$R_L = -\frac{1}{3}R_{out}^0, \tag{2.31}$$

$$X_L = -X_{out}^0. \tag{2.32}$$

Figure 2.7 gives a graphical illustration for the main problem that this approach faces to prove its legitimacy. For a certain feedback elements combination, we assume that the black line represents the approximated relation between the output immittance real part and output amplitude. On the one hand, if the optimum combination is placed instead,

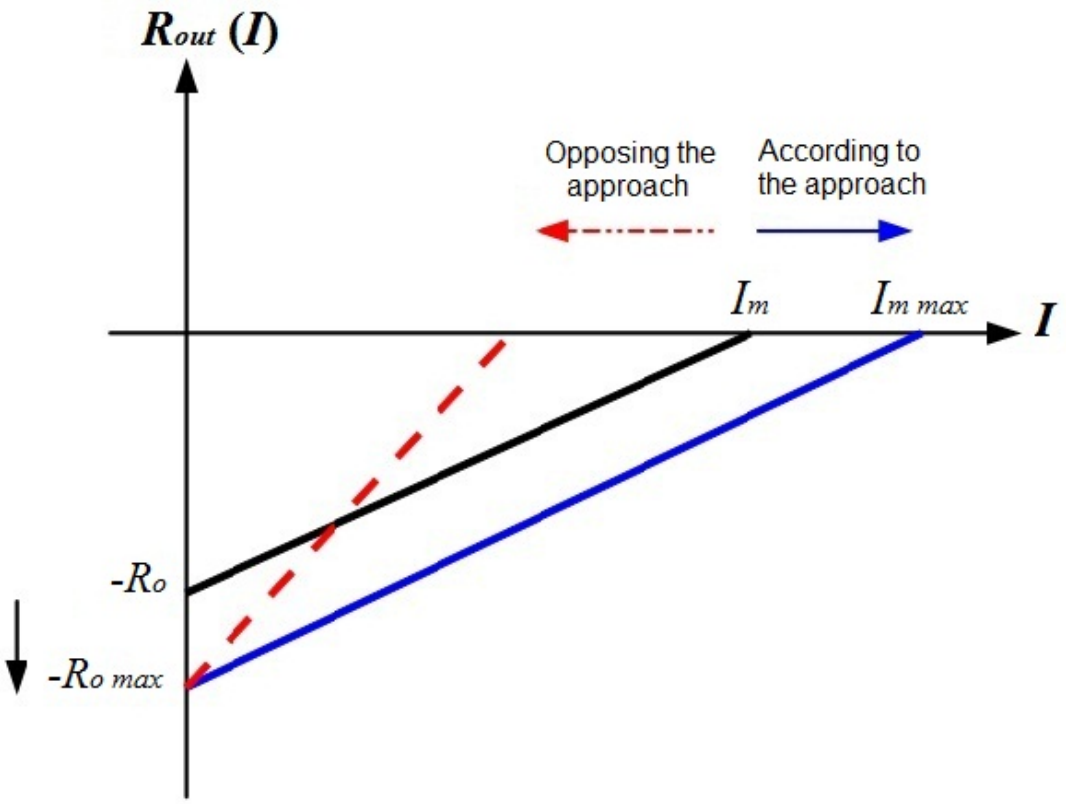

Figure 2.7: The small-signal output resistance R_{out} as a function of current amplitude I. The black line shows $R_{out}(I)$ based on a nonoptimal feedback design. The blue line shows where $R_{out}(I)$ is supposed to shift when $-R_{out}(0)$ is maximized (according to Maeda's approach). The red line shows another possibility that $R_{out}(I)$ could be if $-R_{out}(0)$ is maximized.

then this line is assumed to be shifted as the blue line according to this approach. As a result, both oscillation amplitude and output power will increase. But on the other hand, it has not been proven yet whether the *maximum* negative small-signal resistance (or conductance in other examples) provides *maximum* large signal negative resistance (or conductance) and, consequently, *maximum* amplitude of oscillation or not. So the mentioned relation may also behave as the red dashed line in the same figure, providing less oscillation amplitude and less output power. In the next chapter we will deal with this problem, and examine the oscillator output power when $R_{out}(0)$ or $G_{out}(0)$ is varied on the basis of feedback elements variation.

3. EVALUATION OF "MAXIMUM SMALL-SIGNAL NEGATIVE RESISTANCE/CONDUCTANCE" APPROACH

This chapter is divided into two parts, computer simulations and laboratory measurements. In the computer simulations part, we present a systematic method, carried out on a common example of oscillator circuits, to evaluate the approach that aimed to maximize the output power using the maximum negative resistance/conductance optimal design. The main goal here is to compare between the oscillator output power P_{out} and its corresponding output small-signal resistance/conductance ($R_{out}(0)$ or $G_{out}(0)$) when oscillator's feedback capacitors (C_1, C_2, C_r) are varied. The different combinations of the feedback capacitors can provide us with the optimal design. The resonator inductor L_r is kept at a fixed value that provides high unloaded quality factor Q, since typically it is not possible to vary L_r on a wide range and maintain its high Q at the same time. The main research method was based on designing a BJT Clapp oscillator with a series resonator, and the load was connected either in series or in parallel to the amplifier network. The negative resistance/conductance analysis was applied from the load side. Then the feedback capacitors were varied to find out the corresponding output small-signal negative resistance or conductance. Next, the optimum load value was chosen according to the Gewartowski approach (see equations (2.24) and (2.26)), and the output power was recorded. Finally, the output negative small-signal resistance/conductance was compared to the output power.

In the laboratory measurements part (section 3.2), we designed two Clapp oscillators having the same configurations as in computer simulations part, where one of them was connected to parallel load and the other was connected to series load. For the parallel-load circuit, two feedback combinations were tested, one that supposed to deliver the maximum output power, and the other one that supposed to have the maximum negative conductance (according to simulation results). Then we compared between the two combinations regarding the measured output power. For the series-load circuit, we did the same, but in addition, we plotted the whole output power curve as a function of the feedback capacitors. Then we extracted from this curve, the previously mentioned two combinations and compared between them.

3.1 Computer simulations

Two oscillator circuits were designed and simulated by “Advanced Design System (ADS) 2009” from Agilent Technologies [16]. The first one is connected to a parallel oriented load, where the load is directly in parallel to the amplifier output port. Figure 3.1 shows the placement of the load with respect to both amplifier and feedback networks. The same circuit can be redrawn in more simplified way, as shown in Figure 3.2. The second circuit is connected to a series oriented load, where the load is connected between the amplifier output positive terminal and the feedback input positive terminal, as shown in Figure 3.3 and Figure 3.4.

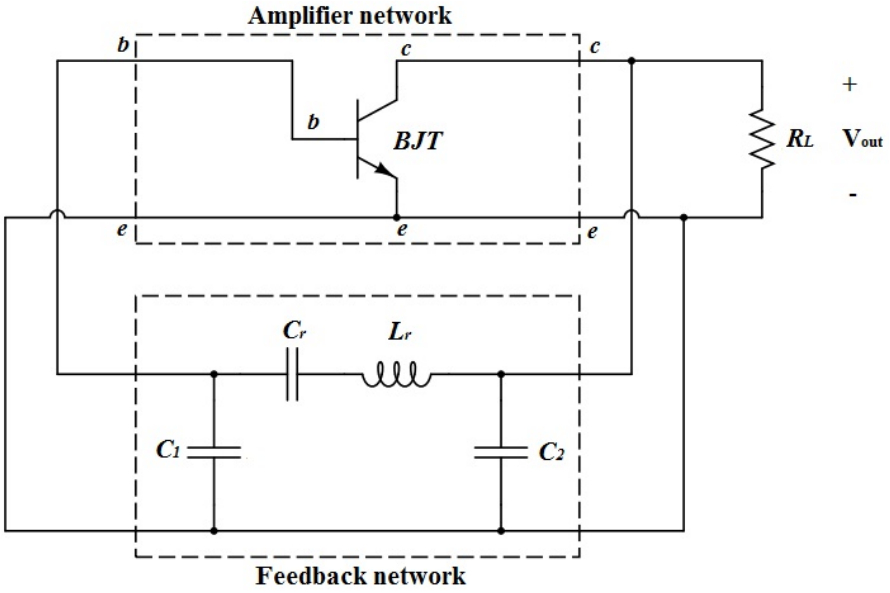

Figure 3.1: A common emitter BJT Clapp oscillator having a π-type feedback network, and connected to a parallel load. The load is connected between transistor collector and emitter nodes. Biasing circuit is omitted.

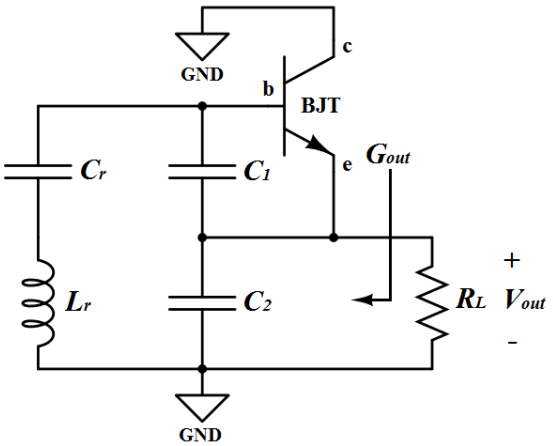

Figure 3.2: Same oscillator circuit as in Figure 3.1, but the components were rearranged in a more simple way, and the collector node is grounded. Output conductance G_{out} is shown.

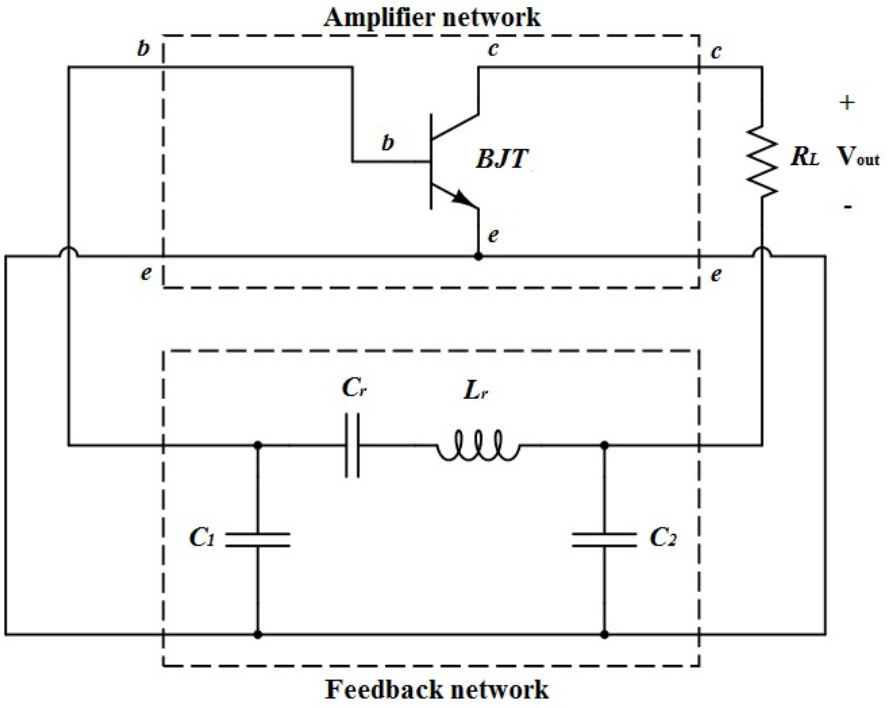

Figure 3.3: A common emitter BJT Clapp oscillator having a π-type feedback network, and connected to a series load. Biasing circuit is omitted.

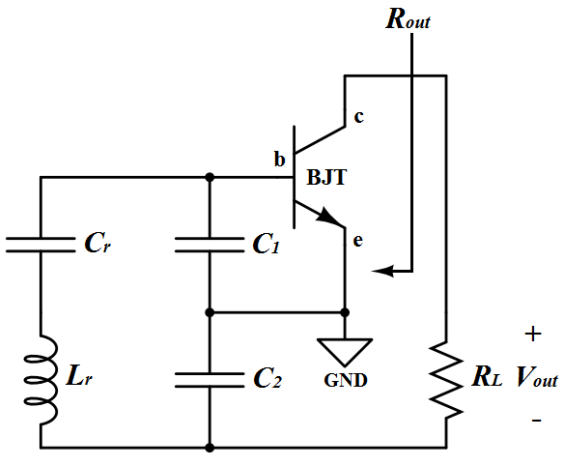

Figure 3.4: Same oscillator circuit as in Figure 3.3, but the components were rearranged in a more simple way, the emitter node is grounded. Output resistance R_{out} is shown.

For each of the two circuits, one procedure was performed to find P_{out} and the corresponding $G_{out}(0)$ or $R_{out}(0)$ for every change of the feedback elements capacitors. During this procedure, the oscillation frequency was kept constant at 100.0 $\pm$ 0.5 MHz by means of properly adjusting values of C_r, and $|G_{out}(0)|/G_L$ (or $|R_{out}(0)|/R_L$) ratio was kept constant at its optimal value (3.0 $\pm$ 0.1). The following flow chart shown in Figure 3.5 summarizes the whole simulation procedure.

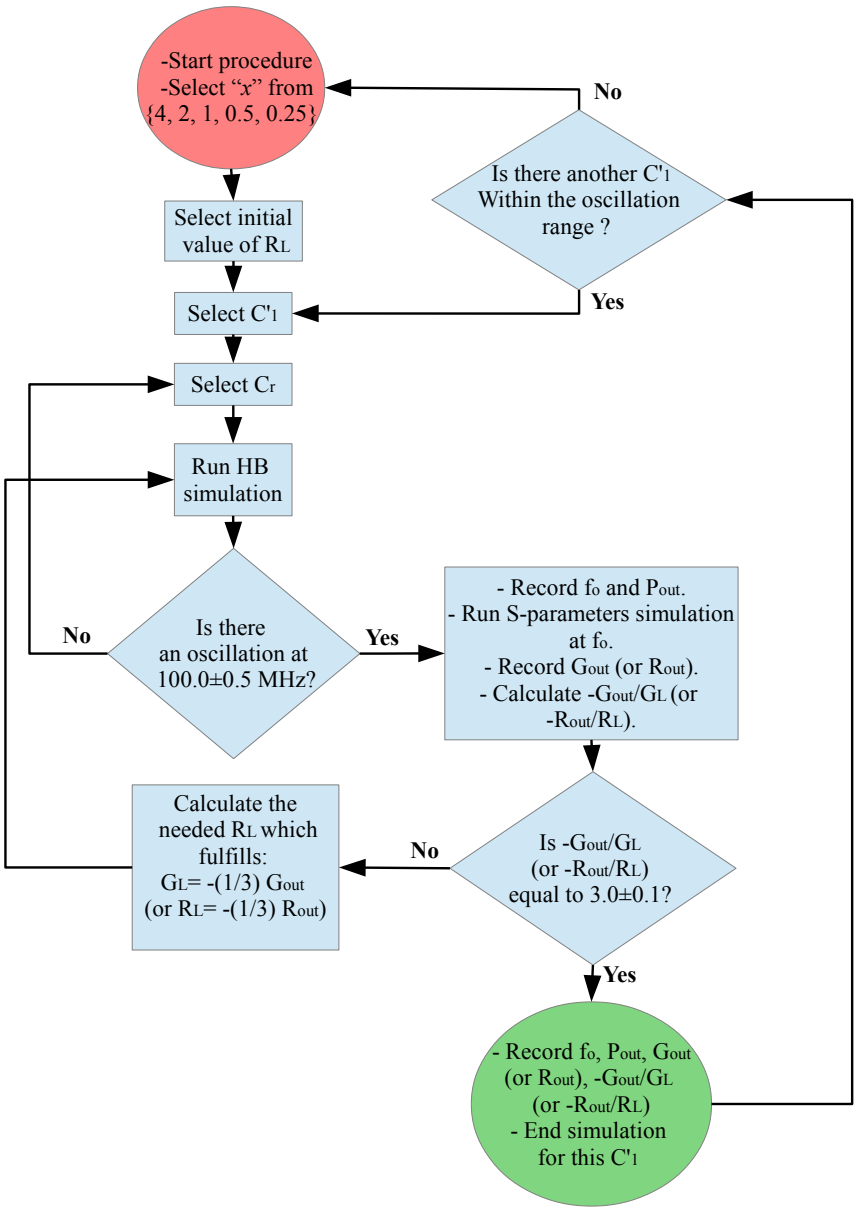

Figure 3.5: The simulation procedure for the 100 MHz Clapp oscillator to obtain P_{out} and G_{out} (or R_{out}). This chart is for both load orientations (parallel and series), where $x = C_1'/C_2'$.

3.1.1 Parallel load circuit

The simulated Clapp oscillator schematic circuit is shown in Figure 3.6. Its inverting amplifier network consisted of a common emitter NPN BJT from "MPS918" type [12]. This BJT was biased at a collector-emitter voltage $V_{CE} = 5$ V and a collector current $I_C = 20$ mA, using a biasing circuit consisted of two resistances $R_1 = 15.04$ kΩ and $R_2 = 4.96$ kΩ of total 20 kΩ. The load R_L was connected between collector and emitter. The oscillator's feedback network was a π-type network, and consisted of a series resonator

and a phase shifter. The resonator was formed by a resonator inductor L_r connected in series to a resonator (tuning) capacitor C_r. The resonator inductor was kept constant[1] at 500 nH, while C_r was slightly varied[2] to tune for 100.0 $\pm$ 0.5 MHz oscillation frequency. The phase shifter consisted of two coupling capacitors C_1 and C_2, to provide a positive feedback, or in other words, to provide basically the other 180 $^\circ$ phase shift so that the total loop phase shift is zero or 360 $^\circ$. For simplicity, the relation between the coupling capacitances was defined by the ratio $x = C_1'/C_2'$, where C_1' and C_2' were defined as:

$$C_1' = C_1 + C_{be}, \tag{3.1}$$

$$C_2' = C_2 + C_{ce}, \tag{3.2}$$

where C_{be} and C_{ce} are the base-emitter and collector-emitter capacitances,[3] respectively.

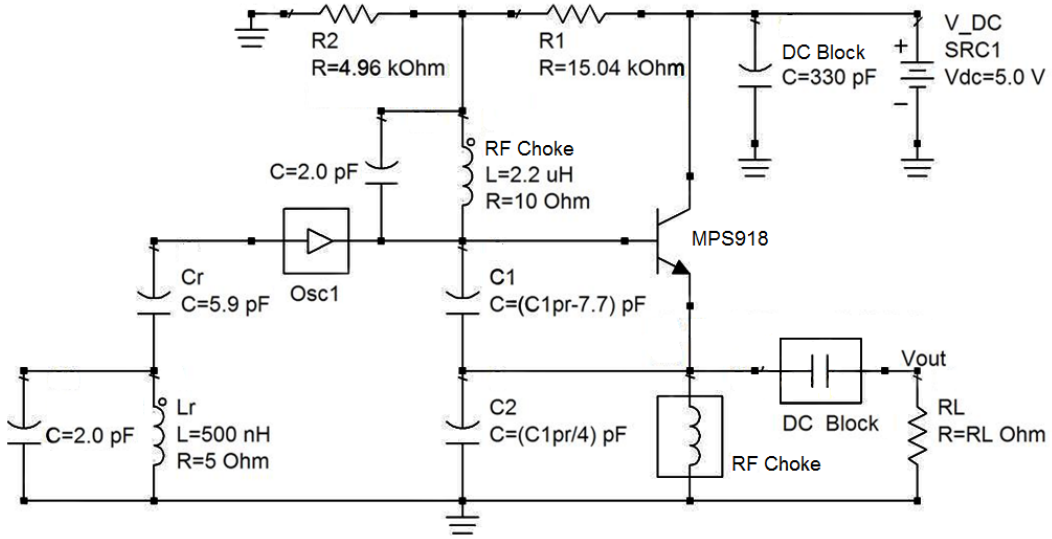

Figure 3.6: Clapp oscillator schematic circuit connected to parallel load (biasing circuit is included). A "harmonic balance" simulation was carried out to test f_o and P_{out}. Then an "S-parameters" simulation was carried out to test $G_{out}(0)$. The current components' values deliver the maximum output power for $x = 4$ (See "Appendix A": Table A.1 at $C_1' = 26$ pF).

For each value of x, the capacitance C_1' was varied within the range of 8 to 200 pF with a suitable steps. At every value of C_1', three consequent simulation steps were performed. First, a "harmonic balance" simulation was done for the circuit shown in Figure 3.6 to adjust the oscillation frequency at 100.0 $\pm$ 0.5 MHz[4] by selecting a suitable C_r value. While an "initial" load was connected, for the fact that the load has no significant effect

[1] At low Values of C_1' and C_2', the resonator inductor value exceeded 500 nH to maintain oscillation frequency at 100 MHz.

[2] At low Values of C_1' and C_2', the resonator capacitor was increased significantly to keep the oscillation frequency at 100 MHz. Thus, the oscillator in this case was considered a Colpitts oscillator.

[3] During simulations, the capacitance C_{be} was assumed to be equal to 7.7 pF [11], while C_{ce} was ignored.

[4] See "Appendix A" for frequency values.

on the frequency. We take here an example from "Appendix A" tables for $C_1' = 26$ pF and $x = 4$ for more clarification. The harmonic balance simulation was run with an initial load of 90 Ω, while C_r was slightly varied until it reached 5.9 pF, which produces an oscillation at $f_o = 99.7$ MHz. Thus the frequency was adjusted, and we did not have to record the output power value that obtained from this step.

In the second step, the one port small-signal negative conductance analysis was applied, where an "S-parameters" simulation was run to record the small-signal output negative conductance for the same circuit, after assigning the value of C_r. The circuit configuration in Figure 3.6 was the same except that the load was replaced by a 50-Ω termination. In our example, the tested negative conductance was -32.03 mS. Then, the optimum load was calculated according to equation (2.24), and it was $3/(32.03\text{ mS}) \approx 93.66\Omega$. The third and last step was a repetition of the first one, but with connecting the optimum load calculated in the second step. The goal was to test the oscillator output power. For our example, the fundamental component of the output power was recorded (18.189 dBm) along with the oscillation frequency (99.8 MHz).

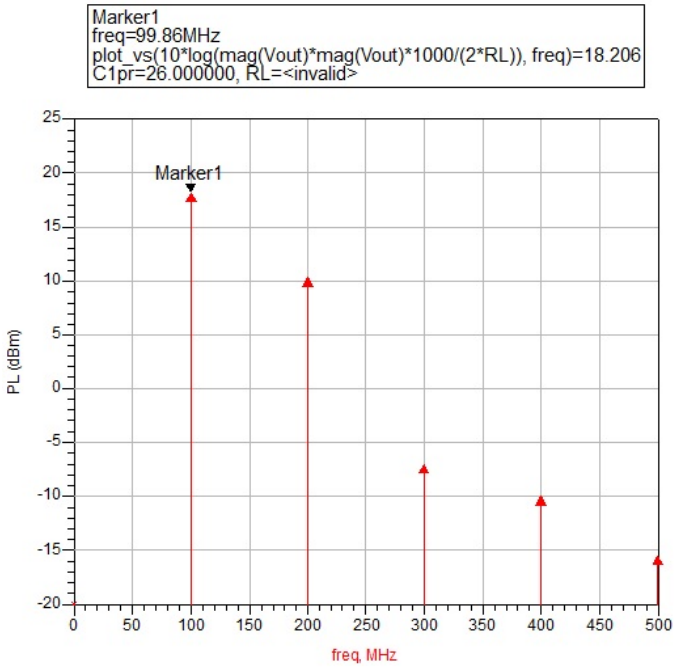

Figure 3.7: An example of the simulated output power spectrum results from the harmonic balance simulation, for $C_1' = 26$ pF and $R_{Lopt.} = 95\ \Omega$.

Notice that the optimum load was different from the initial load and leads to a slight deviation in frequency (0.1 MHz) between the first and last step. Therefore, these steps might be repeated until we reach a constant frequency through all the procedure. After two more iterations, more accurate results have been obtained; the final optimum load was 95 Ω, which delivers 18.206 dBm at 99.9 MHz, as shown in Figure 3.7. While $G_{out}(0)$ was -31.51 mS and $|G_{out}(0)|/G_L = 2.99$. By the end of these three steps

we have obtained one point $(G_{out}(C_1'), P_{out}(C_1'))$ corresponding to a certain value of C_1'. The whole procedure was repeated for all C_1' values within the specified range. Then, a different x value was selected and the same work was done for $x = 4, 2, 1, 1/2$, and $1/4$.

3.1.2 Series load circuit

For the Clapp oscillator configuration having a series oriented load, we tried first to analyze the circuit using the negative conductance concept, but we could not attain any oscillation at the output if we connect a load having $G_L = -\frac{1}{3}G_{out}(0)$. Therefore, we have applied the negative resistance analysis for this circuit. So the same procedure as in the previous section was done except that the small-signal initial output resistance was tested instead. Figure 3.8 shows the schematic circuit used for "harmonic balance" simulation. The same circuit is also used for "S-parameters" simulation by replacing the load by a 50-Ω termination. The biasing circuit was having $R_1 = 15.29$ kΩ, $R_2 = 4.71$ kΩ, and a DC source $V_{DC} = 5.2$ V. This biasing circuit ensured the same quiescent point.

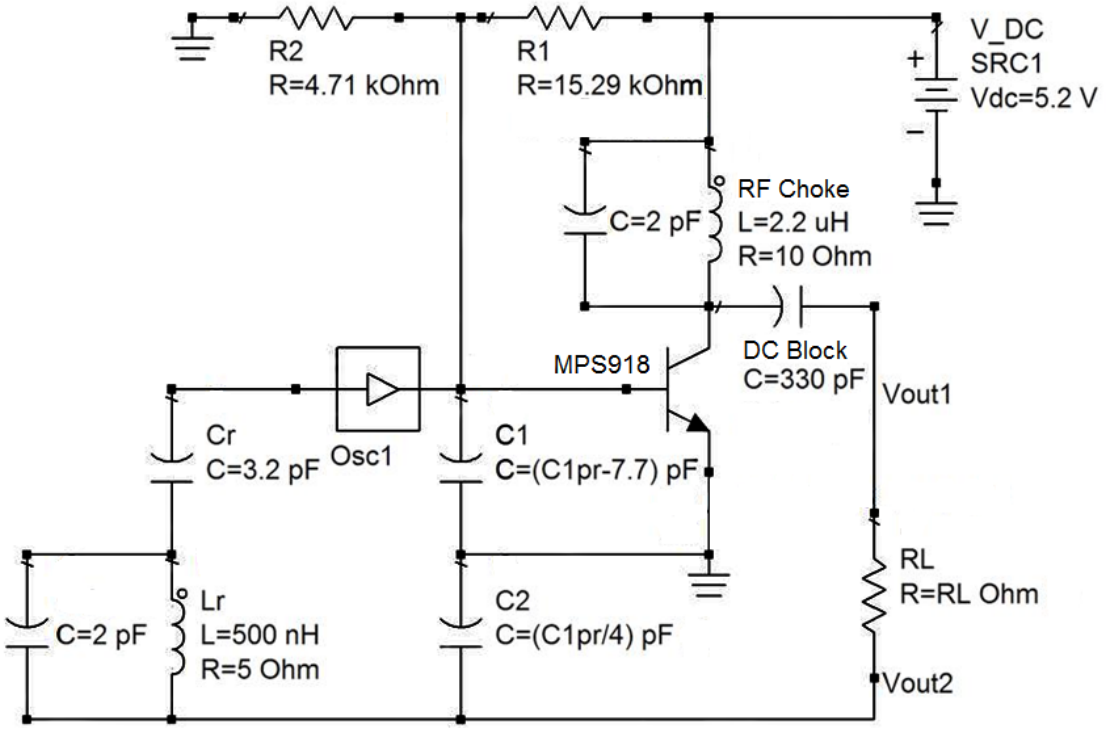

Figure 3.8: Clapp oscillator schematic circuit connected to series load (biasing circuit is included). A "harmonic balance" simulation was carried out to test f_o and P_{out}. Then an "S-parameters" simulation was carried out to test $R_{out}(0)$. Output voltage is $V_{out} = V_{out1} - V_{out2}$. See "Appendix B": Table B.2, for the choices of C_1' and R_L, and the corresponding results.

3.1.3 Results and discussion

For the Clapp oscillator configuration having a parallel oriented load, numerical results are given in "Appendix A", and plotted by Matlab as shown in Figure 3.9. From this figure

we observe that the maximum output power *was not delivered* at the maximum negative conductance. For example, if we look at a specific case as shown in Figure 3.10 for $x = 1/2$, we realize that at $C_1' = 60$ pF, the maximum negative conductance ($G_{out}(0) = -146$ mS) was obtained and has delivered output power level at 3.3 dBm. At the same time, at $C_1' = 15$ pF, the maximum output power was 19.1 dBm for a corresponding negative conductance $G_{out}(0) = -41$ mS, i.e, less than one third of its maximum value. In other words, the maximum values of the output power and negative small-signal conductance magnitude were not vertically aligned. Table 3.1 shows a comparison between maximum output power and maximum negative conductance for different x ratios.

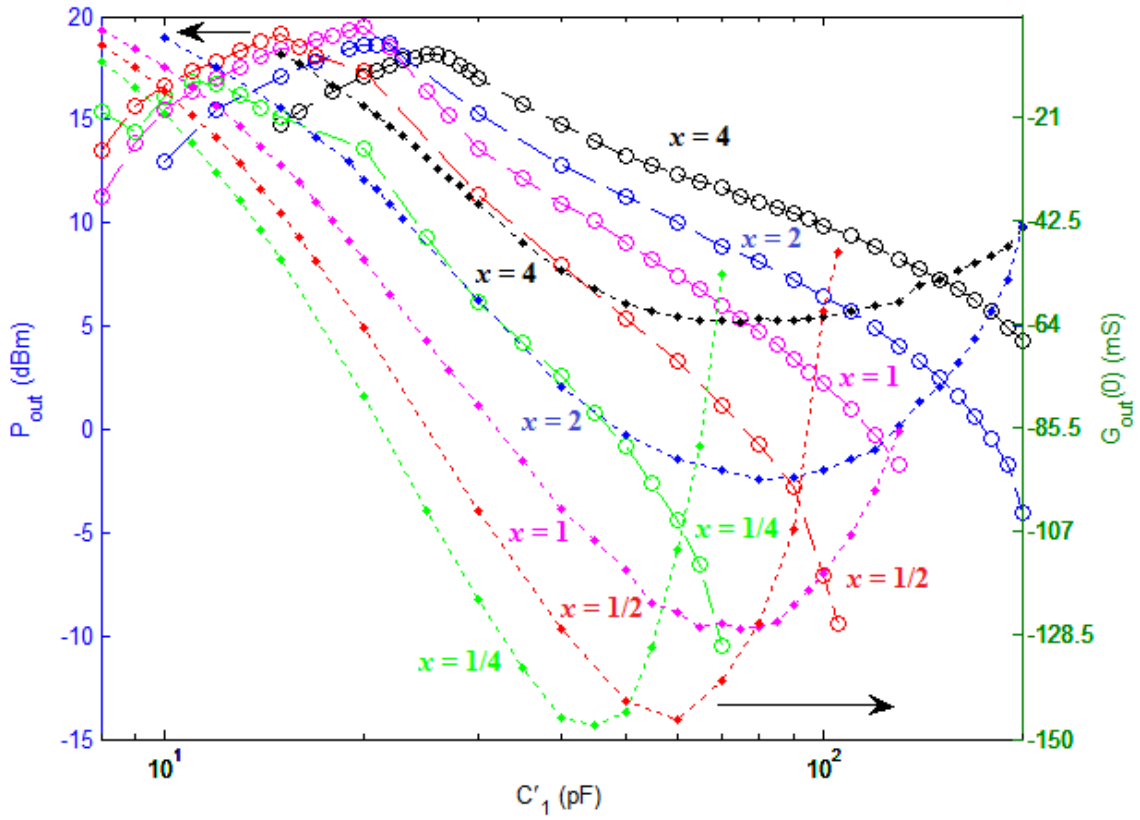

Figure 3.9: Simulated oscillator output power P_{out} (dashed lines) and initial small-signal output negative conductance $G_{out}(0)$ (dotted lines) over a range of C_1' from 8 to 200 pF with various x ratios. These results are for the parallel oriented load circuit, where $G_L = -1/3G_{out}(0)$.

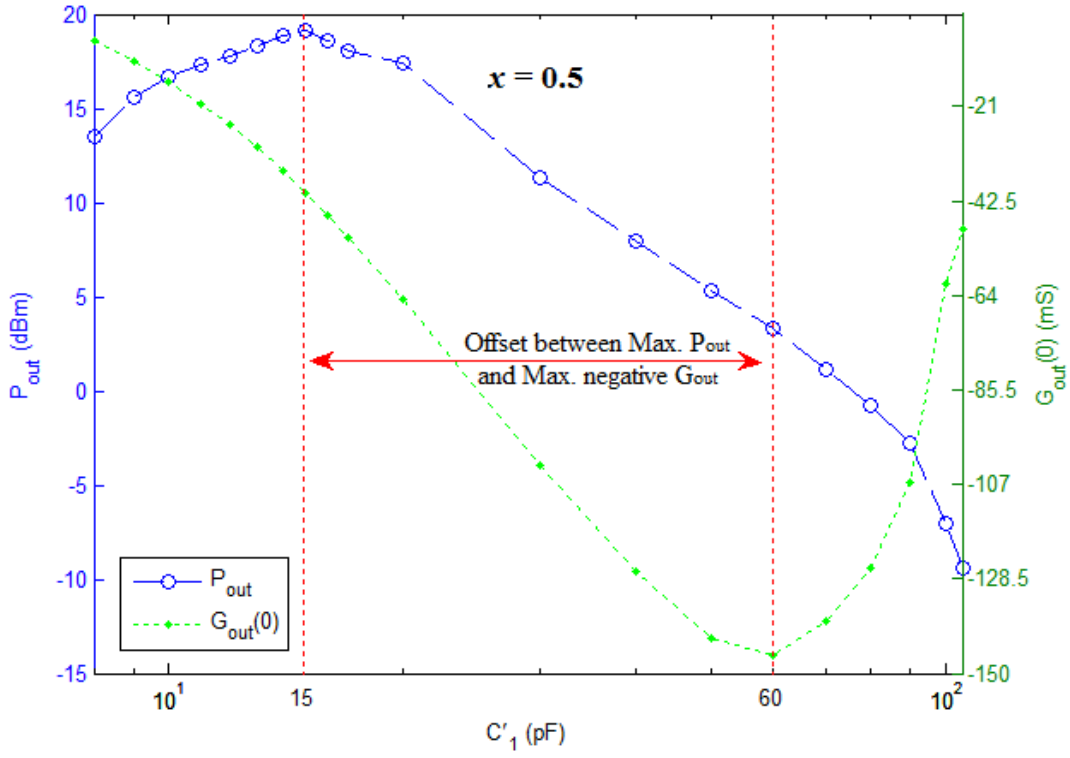

Figure 3.10: Simulated comparison between two C_1' values at $x = 0.5$: for $C_1' = 15$ pF one obtains maximum output power while for 60 pF one obtains maximum negative conductance. C_1' is varied from 8 to 105 pF.

Table 3.1: Comparison between two C_1' values (for every x): one gives maximum P_{out}, while the other one gives maximum negative G_{out}, for oscillator with parallel load.

x	C_1' (pF)	$G_{out}(0)$ (mS)	P_{out} (dBm)
4	26	-32	18.2
	75	-64	11.3
2	22	-39	18.7
	80	-96	8.1
1	20	-50	19.5
	75	-127	5.3
0.5	15	-41	19.1
	60	-146	3.3
0.25	11	-26	16.8
	45	-147	0.8

For plotting G_{out} as a function of the voltage amplitude, first we presume that their relation is represented by a *straight line* according to [7], and hence can be defined by two points. The first point is ($G_{out}(0)$, 0), and the second point is (0, V_m). Where V_m was calculated as follows:

$$P_{out} = \frac{1}{2}\frac{V^2}{R_L} = \frac{1}{2}\frac{(2/3V_m)^2}{R_L}, \tag{3.3}$$

$$V_m = \frac{3}{\sqrt{2}}\sqrt{P_{out}R_L}. \tag{3.4}$$

The resultant $G_{out}(V)$ lines at $x = 4$ and 2 are shown in Figures 3.11 and 3.12, respectively. The lines illustrate the same simulation results from another perspective. In these figures, The red line which has maximum $|G_{out}(0)|$ *is not leading* to maximum V_m while G_{out} magnitude is diminishing. Whereas the blue line *delivers* the maximum output power at its steady-state point (at $V = \frac{2}{3}V_m$) despite of having less $|G_{out}(0)|$. While green lines were resulted from other feedback combinations. More graphs for the remaining x ratios are shown in “Appendix C”.

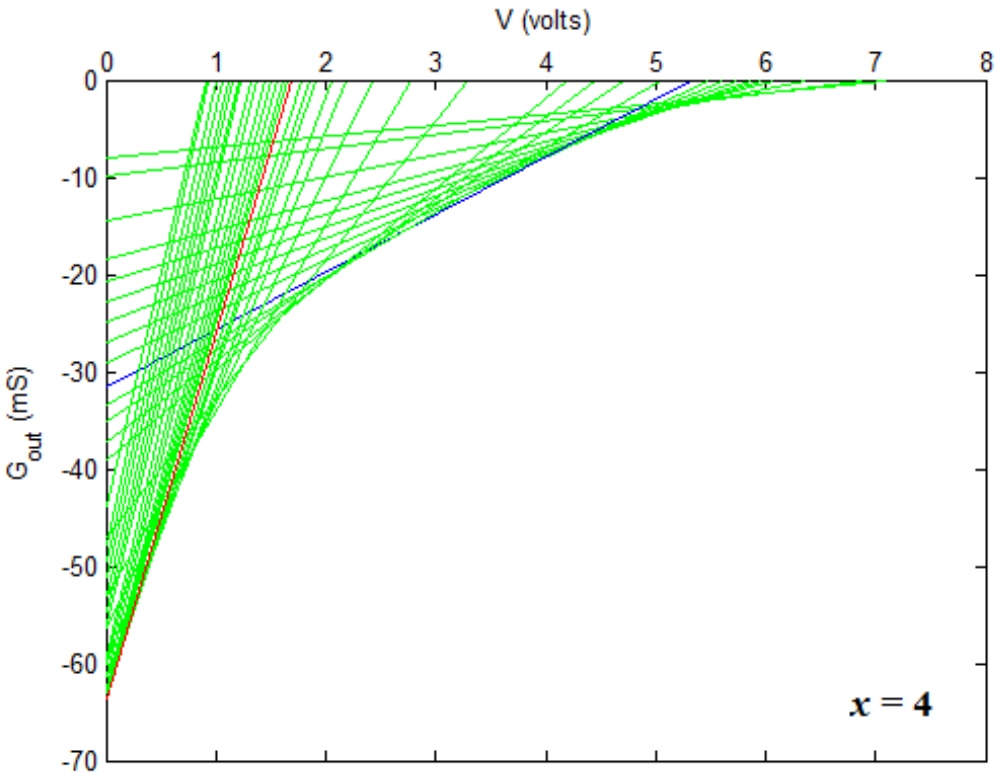

Figure 3.11: Simulation results for the small-signal output conductance G_{out} as a function of V with $x = 4$. a) Blue line: maximum power combination. b) Red line: maximum negative conductance combination. c) Green lines: other combinations.

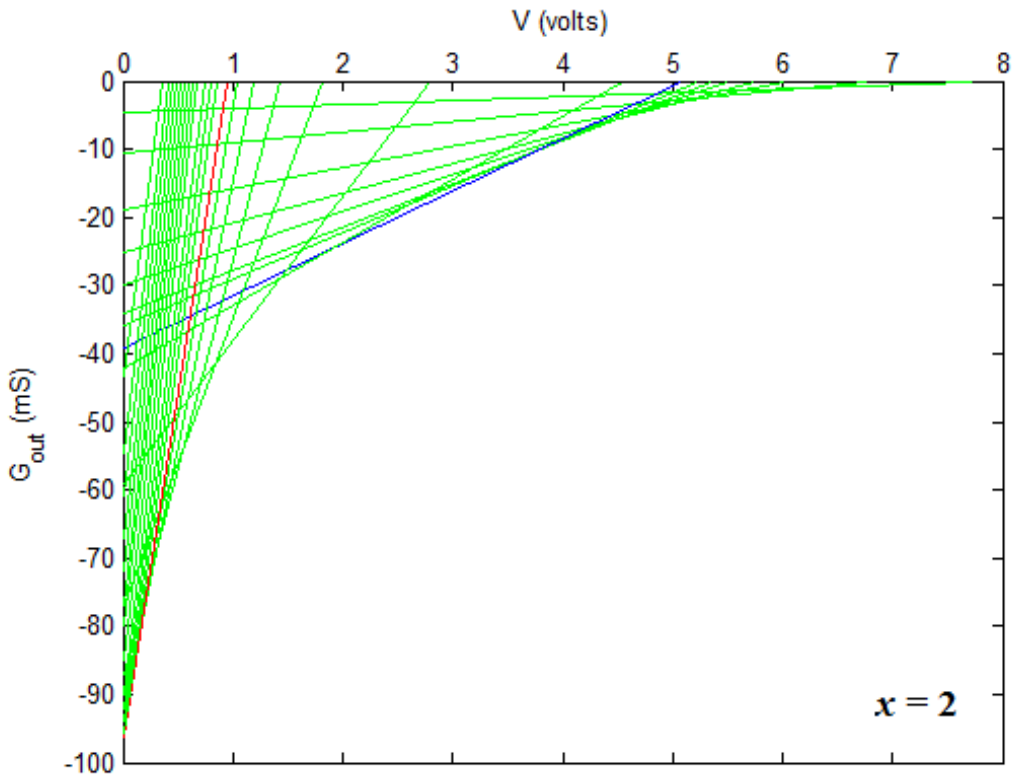

Figure 3.12: Simulation results for the small-signal output conductance G_{out} as a function of V with $x = 2$. a) Blue line: maximum power combination. b) Red line: maximum negative conductance combination. c) Green lines: other combinations.

For the Clapp oscillator configuration having a series oriented load, results are recorded in "Appendix B" and were plotted for $x = 4$, 2, 1, and 0.5[5], as shown in Figure 3.13. Similarly we observe that the maximum output power *was not delivered* at the maximum negative resistance. For example, Figure 3.14 shows a specific case at $x = 2$, where we notice that at $C_1' = 45$ pF, the maximum negative resistance $R_{out}(0) = -1.46$ kΩ was achieved, and has delivered output power level at 10.2 dBm. On the other hand, at $C_1' = 123$ pF, the output power has reached the maximum at 16.5 dBm for a corresponding negative resistance $R_{out}(0) = -368\ \Omega$. Table 3.2 shows a comparison between maximum output power and maximum negative resistance for different x ratios.

[5]Curve $x = 1/4$ could not be plotted because the condition $R_L = -1/3R_{out}(0)$ did not hold for loads within oscillation range.

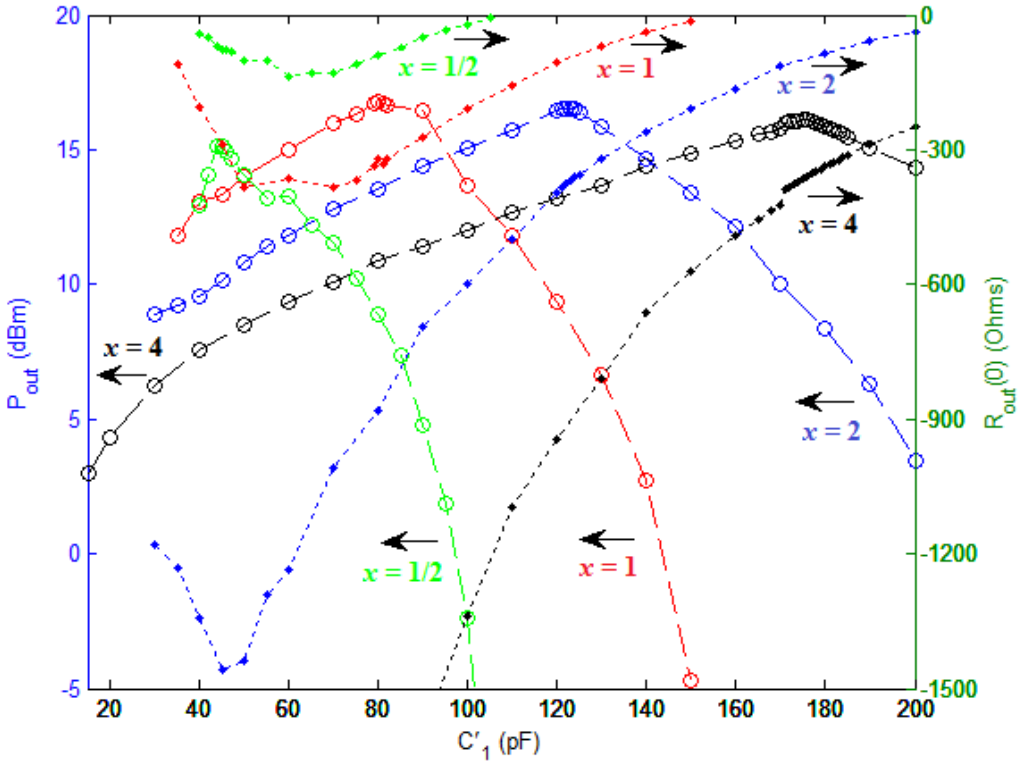

Figure 3.13: Simulated oscillator output power P_{out} (dashed lines) and initial small-signal output negative resistance $R_{out}(0)$ (dotted lines) over a range of C_1' from 15 to 200 pF with various x ratios. These results are for the series oriented load circuit, where $R_L = -1/3R_{out}(0)$.

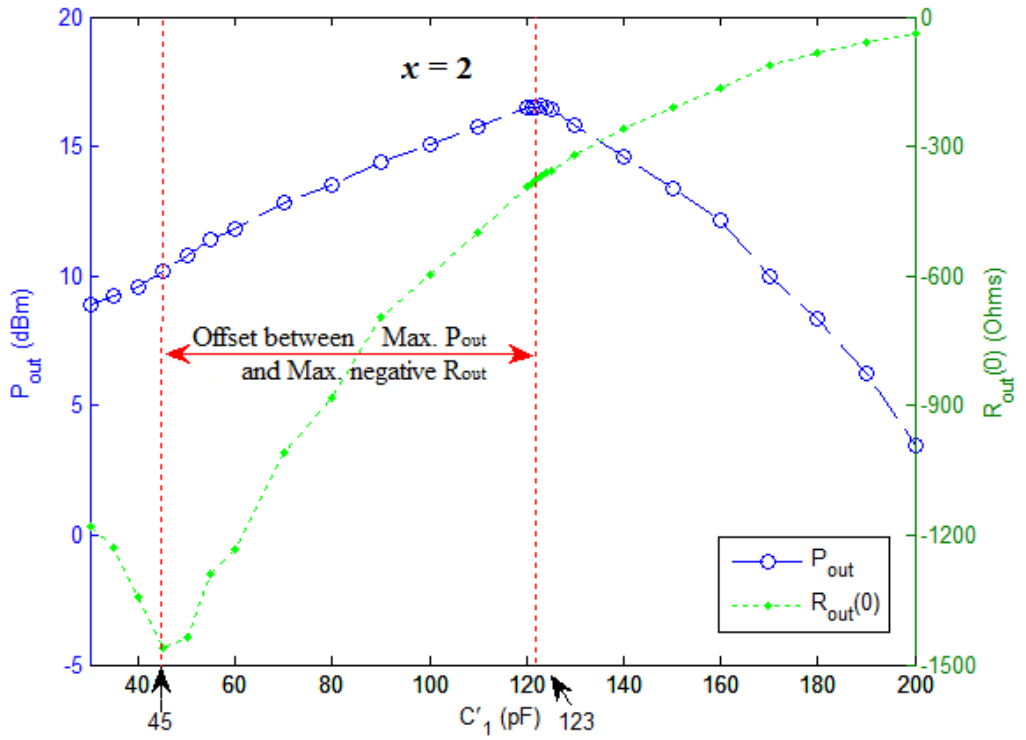

Figure 3.14: Simulated comparison between two C_1' values: for $C_1' = 45$ pF one obtains maximum negative resistance while for 123 pF one obtains maximum output power. C_1' is from 30 to 200 pF.

Table 3.2: Comparison between two C_1' values (for every x): one gives maximum P_{out}, while the other one gives maximum negative R_{out}, for oscillator with series load.

$\boldsymbol{x}$	$\boldsymbol{C_1'}$ (pF)	$\boldsymbol{R_{out}(0)(\Omega)}$	$\boldsymbol{P_{out}}$ (dBm)
4	15	-9445	3.0
	175	-365	16.1
2	45	-1460	10.2
	123	-368	16.5
1	70	-384	16.0
	81	-333	16.7
0.5	45	-76	15.1
	60	-138	13.3

The output resistance R_{out} also can be plotted as a function of the current amplitude I considering a *straight line* relation defined by two points. The first point is ($R_{out}(0)$, 0), and the second point is (0, I_m). Where I_m was calculated as follows:

$$P_{out} = \frac{1}{2} I^2 R_L = \frac{1}{2} (\frac{2}{3} I_m)^2 R_L, \tag{3.5}$$

$$I_m = \frac{3}{\sqrt{2}} \sqrt{\frac{P_{out}}{R_L}}. \tag{3.6}$$

Results of $R_{out}(I)$ lines at $x = 4$ and 2 are shown in Figures 3.15 and 3.16. The red line which has maximum $|R_{out}(0)|$ *is not leading* to maximum V_m while R_{out} magnitude is diminishing. The blue line *delivers* the maximum output power at its steady-state point (at $A = \frac{2}{3} A_m$) although it has much less $|R_{out}(0)|$. More graphs for the remaining x ratios are shown in "Appendix D".

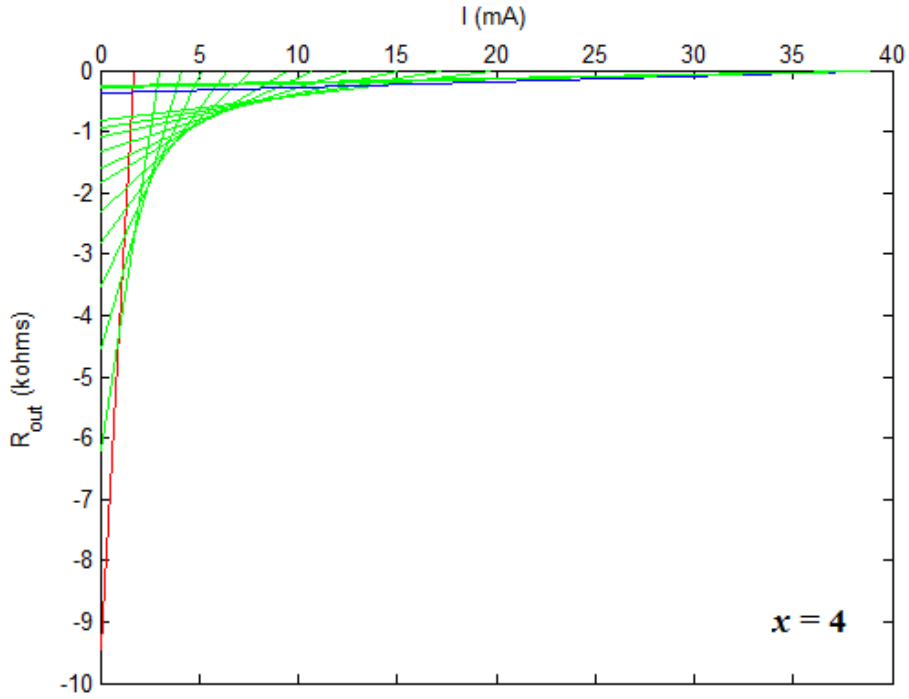

Figure 3.15: Simulation results for the small-signal output resistance R_{out} as a function of I with $x = 4$. a) Blue line: maximum power combination. b) Red line: maximum negative resistance combination. c) Green lines: other combinations.

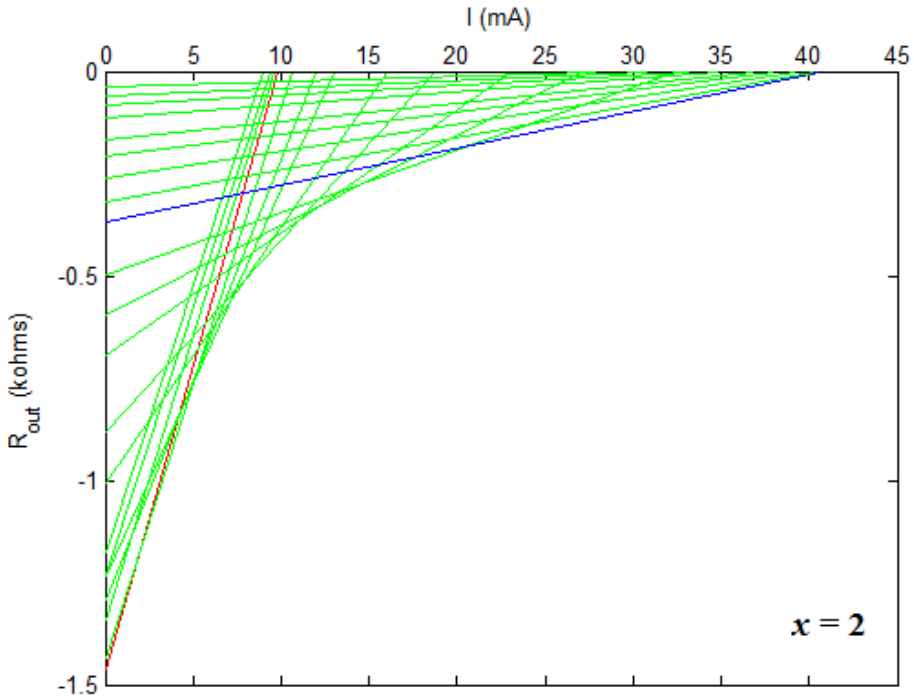

Figure 3.16: Simulation results for the small-signal output resistance R_{out} as a function of I with $x = 2$. a) Blue line: maximum power combination. b) Red line: maximum negative resistance combination. c) Green lines: other combinations.

The results show a significant disagreement with the approach - under examination - which aimed to maximize oscillator output power. So, maximizing negative small-signal resistance or conductance at the output port of the active part *does not guarantee* delivery of maximum output power. Another observation from the results is that the parallel connected loads deliver more output power than the series ones if the feedback elements are freely selected. Figure 3.17 illustrates a comparison between parallel and series load connections. It is shown that parallel connection gives 18.7 and 18.2 dBm, while the series one gives 16.5 and 16.1 dBm as peak powers, for $x = 2$ and 4, respectively. Also, we notice that the parallel load delivers more power at lower C_1' and C_2' values, whereas the series load delivers more power at higher C_1' and C_2' values.

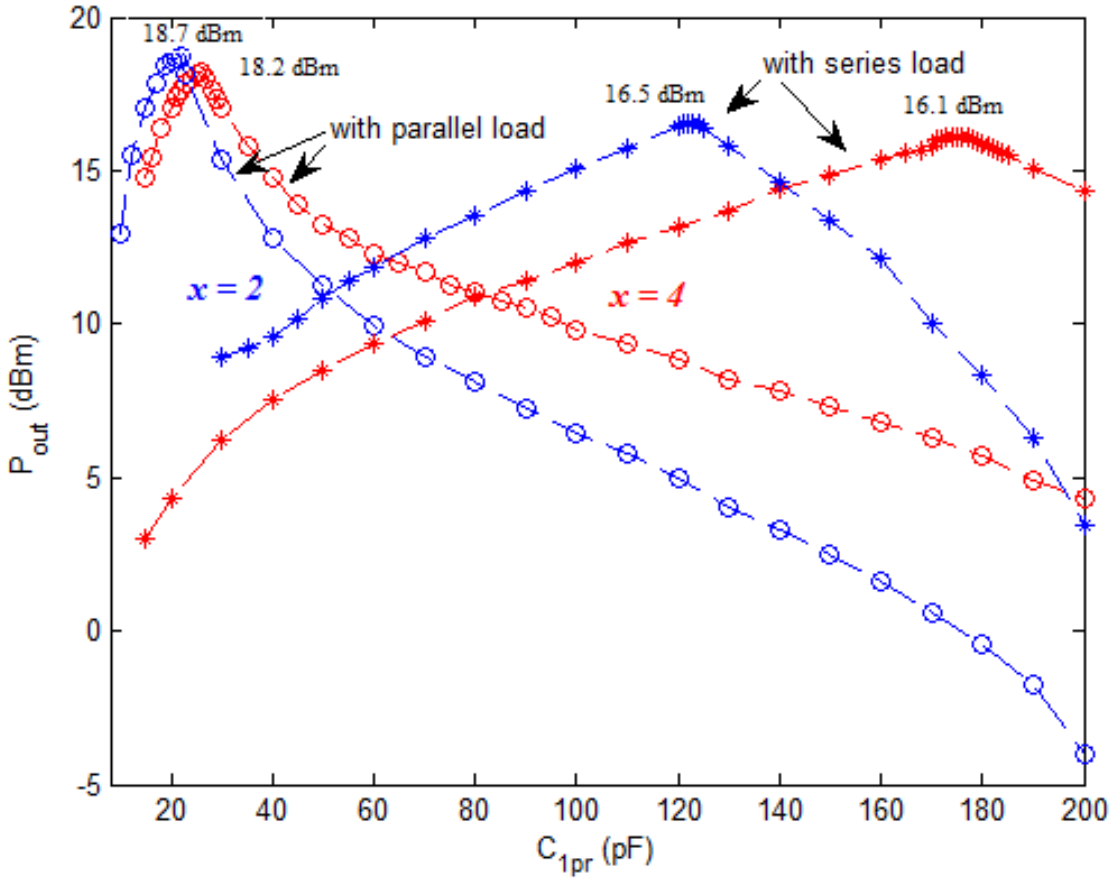

Figure 3.17: Simulated comparison of Output power results of parallel and series oriented load oscillators for $x = 2$ (blue curves) and $x = 4$ (red curves).

3.2 Laboratory measurements

This section is a continuation to the work done in section 3.1. We aim to verify practically the results obtained by simulations. The following laboratory measurements were done using a spectrum analyzer of model “E4407B” from Agilent technologies [17]. The spectrum analyzer was set to a Resolution Bandwidth (RBW) of 300 kHz, Video Bandwidth

(VBW) of 300 kHz and Reference level equal to 15 dBm. An input DC voltage source was used along with a series ammeter for transistor biasing.

3.2.1 Parallel load circuit

An oscillator circuit was designed, as per the schematic shown in Figure 3.6, on a printed circuit board (PCB) to perform a power measurement test for two feedback elements combinations. The first combination was the one that delivered the maximum output power. The second one was by which the maximum conductance has occurred. The load was connected in parallel and the coupling ratio x was equal to two. The two combinations - under test - were as follows:

- The maximum output power combination[6]: $C_1' = 21$ pF, $C_2' = 10.5$ pF, $C_r = 5.6$ pF, $L_r = 500$ nH, and $R_L = 83\ \Omega$.
- The maximum negative conductance combination: $C_1' = 80$ pF, $C_2' = 40$ pF, $C_r = 3.4$ pF, $L_r = 500$ nH, and $R_L = 31\ \Omega$.

The final PCB design is shown in Figure 3.18. Transistor model was “PN3563” which has similar characteristics to “MPS918” [13]. The resonator inductor was formed by an air wounded copper coil, and its specifications is given in “Appendix E”. The remaining circuit components are illustrated in Table 3.3. A 5-V DC source, along with a series ammeter, was connected between the collector node and ground, while the 20-kΩ potentiometer was varied to draw a DC current $I_{CC} = 20.2$ mA, which ensures a collector current $I_C = 20$ mA (see “Appendix F” for biasing settings). The output power was measured by the spectrum analyzer.

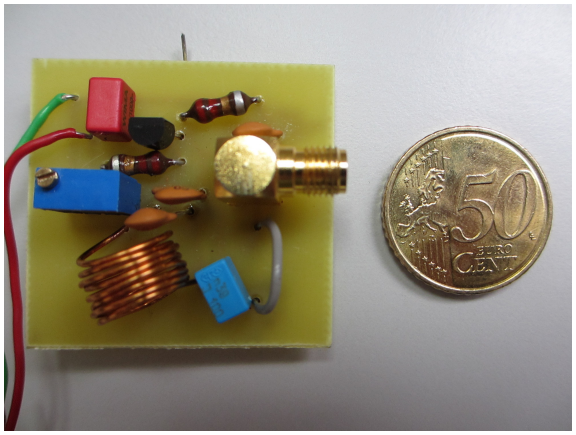

Figure 3.18: The final Clapp oscillator circuit design on a PCB.

[6]This combination provided the second maximum output power on “$x = 2$” curve with $P_{out} = 18.6$ dBm, while the maximum power was 18.7 dBm. It was chosen because their elements’ values have the nearest match to the standard components’ values in the laboratory.

Table 3.3: Components discription for the PCB circuit.

Component	**Specification**
Transistor	PN3563 model
Biasing RF choke	2.2 μH
Output RF choke	2.2 μH
Source DC Block	330 pF
Output DC Block	390 pF
Potentiometer	20 kΩ
RF connector	SMA type
Capacitors	Disc Ceramic type

To test the circuit with the maximum power combination, it was difficult to use the simulated capacitor values through the practical test due to the limitation of capacitors standard values in the laboratory. However, the values chosen for test were as close as possible to the simulated ones. So the final values for the combination - under test - was:

- C_1'[7] $= 19.7$ pF, $C_2' = 10$ pF, $C_r = 5.6$ pF, $L_r = 500$ nH, and $R_L = 83.3\ \Omega$.

Based on the simulations, this combination has $G_{out}(0) = -33$ mS. The Load R_L was formed by a series connection of the spectrum analyzer internal resistance (50 Ω) and an external resistor of 33.3 Ω as shown in Figure 3.19.

Test results are illustrated in Figure 3.20, that shows the fundamental and two harmonics components for the spectrum analyzer input power $P_{S.A.}$. From this figure, the measured value of $P_{S.A.}$ was 11.96 dBm at 100.3 MHz. By the following calculations, the output power was deduced:

$$P_{S.A.} = \frac{1}{2}\frac{V_{S.A.}^2}{R_{S.A.}}, \tag{3.7}$$

$$\begin{aligned} V_{S.A.} &= \sqrt{2P_{S.A.}R_{S.A.}} \\ &= \sqrt{(2)\left(\frac{10^{1.196}}{1000}\right)(50)} \\ &= 1.253\ \text{V}, \end{aligned} \tag{3.8}$$

$$V_{S.A} = \frac{R_{S.A}}{R_{S.A} + R_{ex.}}V_{out}, \tag{3.9}$$

[7]The ceramic capacitor used was $C_1 = 12$ pF, assuming $C_{be} = 7.7$ pF.

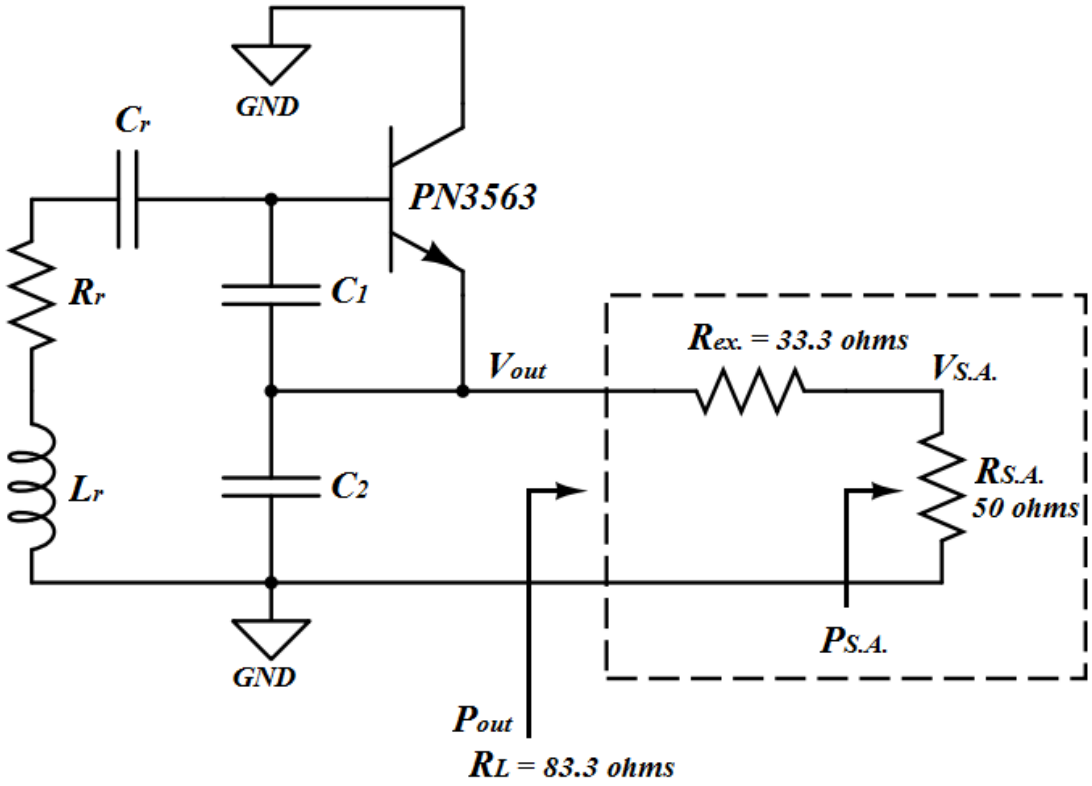

Figure 3.19: Oscillator schematic showing the load formation and connection for the maximum power combination. Biasing circuit is omitted.

$$\begin{aligned} V_{out} &= \frac{R_{S.A} + R_{ex.}}{R_{S.A}} V_{S.A} \\ &= \left(\frac{50 + 33.3}{50}\right)(1.253) \\ &= 2.088 \text{ V}, \end{aligned} \tag{3.10}$$

$$P_{out} = \frac{1}{2}\frac{V_{out}^2}{R_L} = \frac{1}{2}\left(\frac{2.088^2}{83.3}\right) = 26.2 \text{ mW} = 14.18 \text{ dBm}. \tag{3.11}$$

From equation (3.11), the output (or load) power was equal to 14.18 dBm (26.2 mW). Next, we will repeat the same work done using the maximum negative conductance combination.

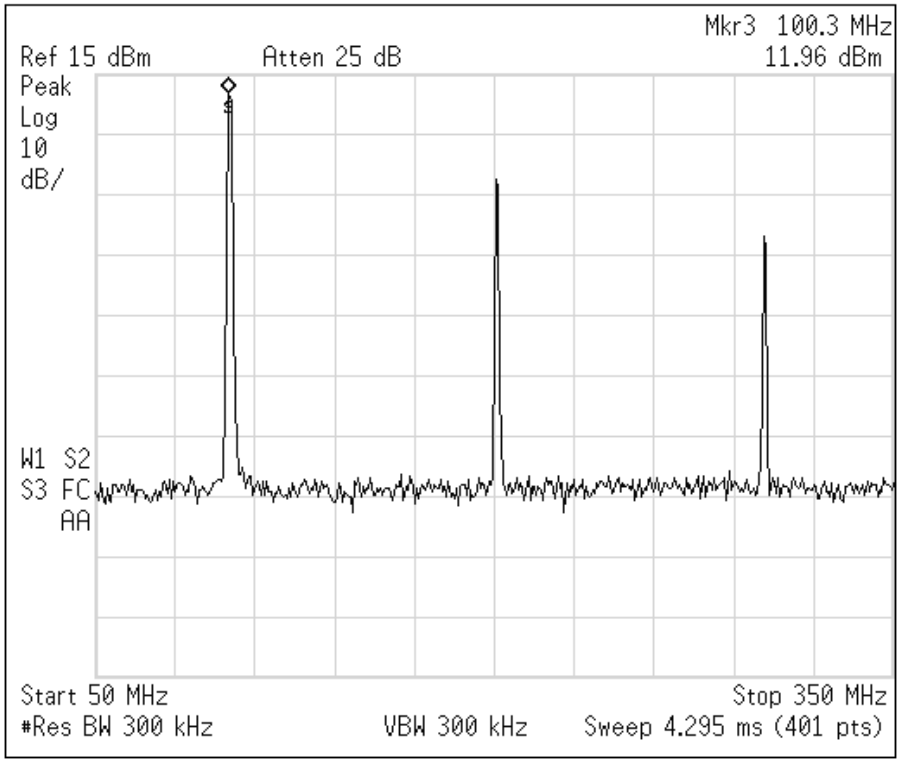

Figure 3.20: Spectrum analyzer screenshot showing the output power for the maximum power combination.

For the maximum negative conductance combination, The following values were used:

- $C_1' = 75.7$ pF, $C_2' = 39$ pF, $C_r = 3.3$ pF, $L_r = 500$ nH, and $R_L = 31\ \Omega$.

From simulation, this combination gives $G_{out}(0) = -96$ mS. The Load R_L was formed by a parallel connection of the spectrum analyzer internal resistance (50 Ω) and an external resistor of 82 Ω as shown in figure 3.21.

Other circuit settings were the same as before. Figure 3.22 shows the fundamental and three harmonics components for the analyzer input power. The measured value of the input power $P_{S.A.}$ was -0.637 dBm at 76.3 MHz. we notice that the frequency has been shifted significantly as C_r value should have been lower than 3.3 pF. However, the output power was much less than maximum power obtained from the other combination. The output power can be deduced from the following calculations:

$$P_{S.A.} = \frac{1}{2}\frac{V_{out}^2}{R_{S.A.}}, \tag{3.12}$$

$$V_{out} = \sqrt{2P_{S.A.}R_{S.A.}} = \sqrt{(2)\left(\frac{10^{-0.0637}}{1000}\right)(50)} = 0.294\ \text{V}, \tag{3.13}$$

$$P_{out} = \frac{1}{2}\frac{V_{out}^2}{R_L} = \frac{1}{2}\left(\frac{0.294^2}{31}\right) = 1.4\ \text{mW} = 1.44\ \text{dBm}. \tag{3.14}$$

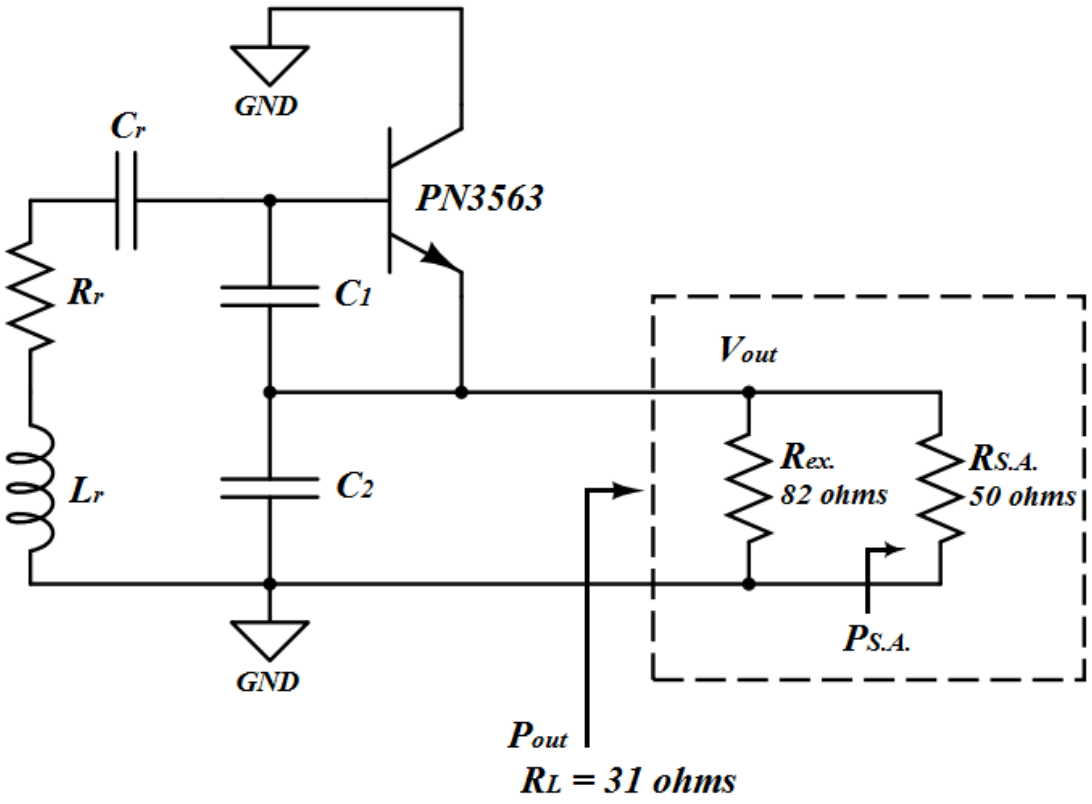

Figure 3.21: Oscillator schematic showing the load formation and connection for the maximum negative conductance combination. Biasing circuit is omitted.

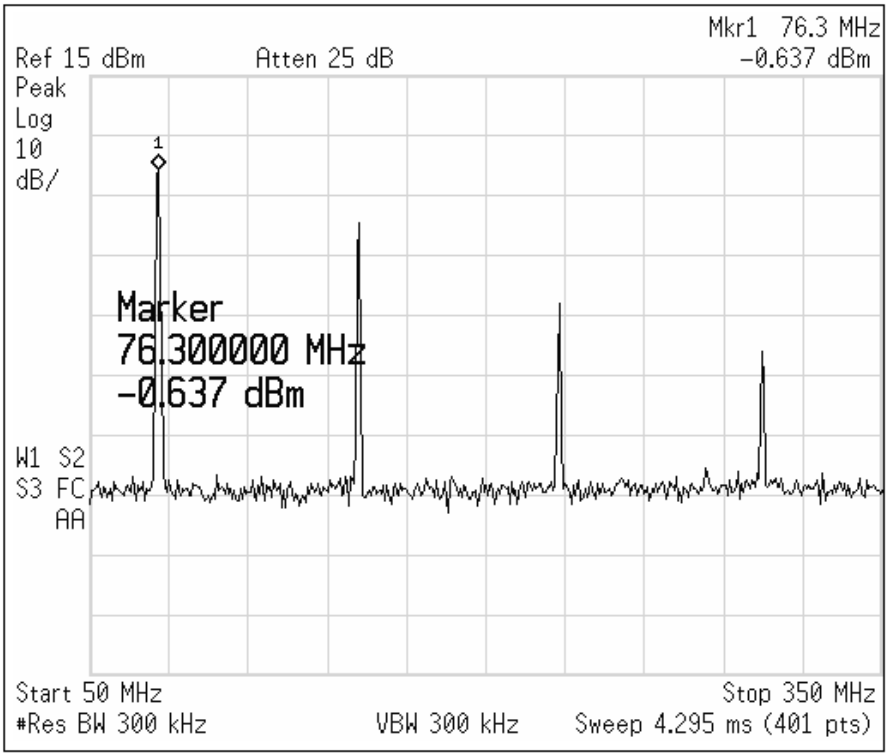

Figure 3.22: Spectrum analyzer screenshot showing the output power for the maximum conductance combination.

From the last equation, the output power was 1.44 dBm, which is much lower than the maximum output power (14.2 dBm) despite having a maximum negative conductance in this case. All in all, the maximum power combination *has practically delivered* higher power than the power delivered by the maximum conductance combination (either the simulated or the laboratory tested one). Table 3.4 summarizes the main results of this section.

Table 3.4: Comparison between simulation and laboratory results for the output power of oscillator with parallel load, at $x = 2$.

		$\boldsymbol{P_{out}}$ (dBm)
Simulation results	Maximum P_{out} combination	18.7
	Maximum G_{out} combination	8.1
Laboratory results	Maximum P_{out} combination	14.2
	Maximum G_{out} combination	1.4

3.2.2 Series load circuit

This is the second part of the laboratory measurements, where we have tested the oscillator circuit that is connected to a series load. Figure 3.23 shows the schematic of the tested circuit, while table 3.5 shows more details about the used components. A 5.2-V DC source was connected along with a series ammeter which was adjusted to read 20.3 mA on its screen using a 20-kΩ potentiometer. Therefore, the quiescent point remained the same at $V_{CEQ} = 5$ V and $I_{CQ} = 20$ mA (see “Appendix F” for biasing settings). The final circuit was built on a solderless breadboard as shown in Figure 3.24.

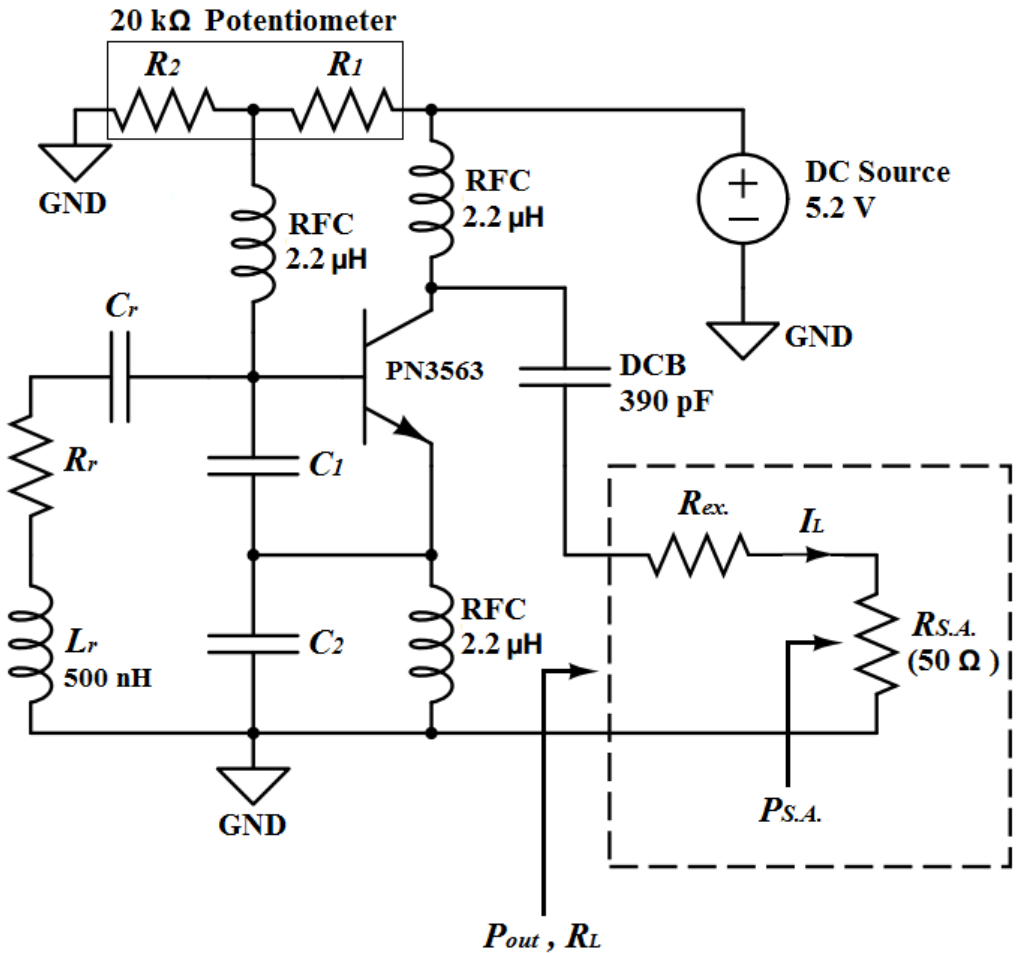

Figure 3.23: Schematic of the tested Clapp oscillator circuit. The load ($R_L = R_{S.A.} + R_{ex.}$) is connected in series. The resistance R_r is the LC-resonator's equivalent series resistance.

Table 3.5: Components discription for the breadboard circuit.

Component	**Specification**
Transistor	PN3563 model
Biasing RF chokes	2.2 μH
Output DC Block	390 pF
Potentiometer	20 kΩ
RF connector	SMA type
Capacitors	Disc Ceramic type
Resonator inductor	500 nH Air-wound copper coil

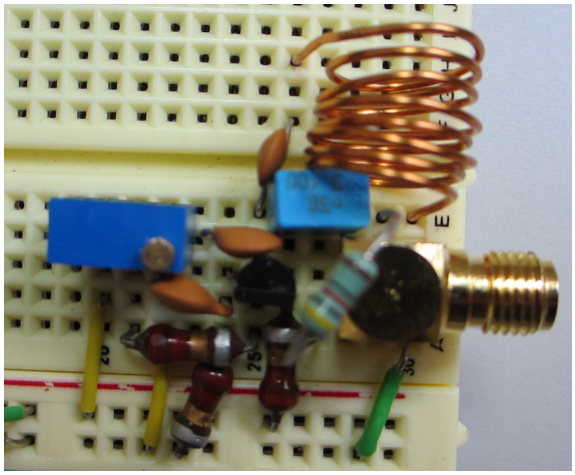

Figure 3.24: The final 70 MHz Clapp oscillator circuit design on a breadboard.

The oscillation frequency was set to 70 MHz instead of 100 MHz, because the tested circuit could not produce oscillations with C_r less than 10 pF. Figure 3.25 shows the simulated circuit with two C_r choices, where at $C_r = 3.3$ pF, the circuit oscillates around 100 MHz. While at $C_r = 10$ pF, the circuit oscillates around 70 MHz. As a result, the simulations done in section 3.1.2 were repeated for one curve only ($x = 2$) at 70 ± 1 MHz to support the Lab. measurements. The new simulation results at 70 MHz are plotted in Figure 3.26 (see “Appendix B” for the recorded numerical results). From this figure, we observe that the maximum output power (16.5 dBm) was delivered at a local negative resistance value $R_{out}(0) = -402\ \Omega$, so the same outcomes illustrated in section 3.1 were obtained at a different frequency.

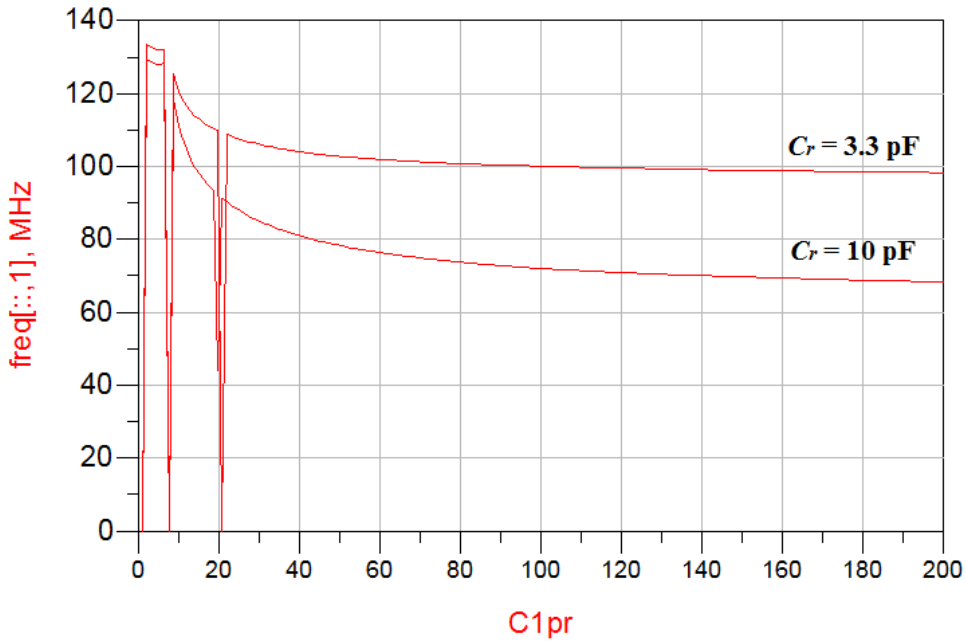

Figure 3.25: Simulation results for f_o over a range of C_1' values at C_r3.3 and 10 pF. The Clapp oscillator is connected to a series 50 Ω load, while $x = 2$.

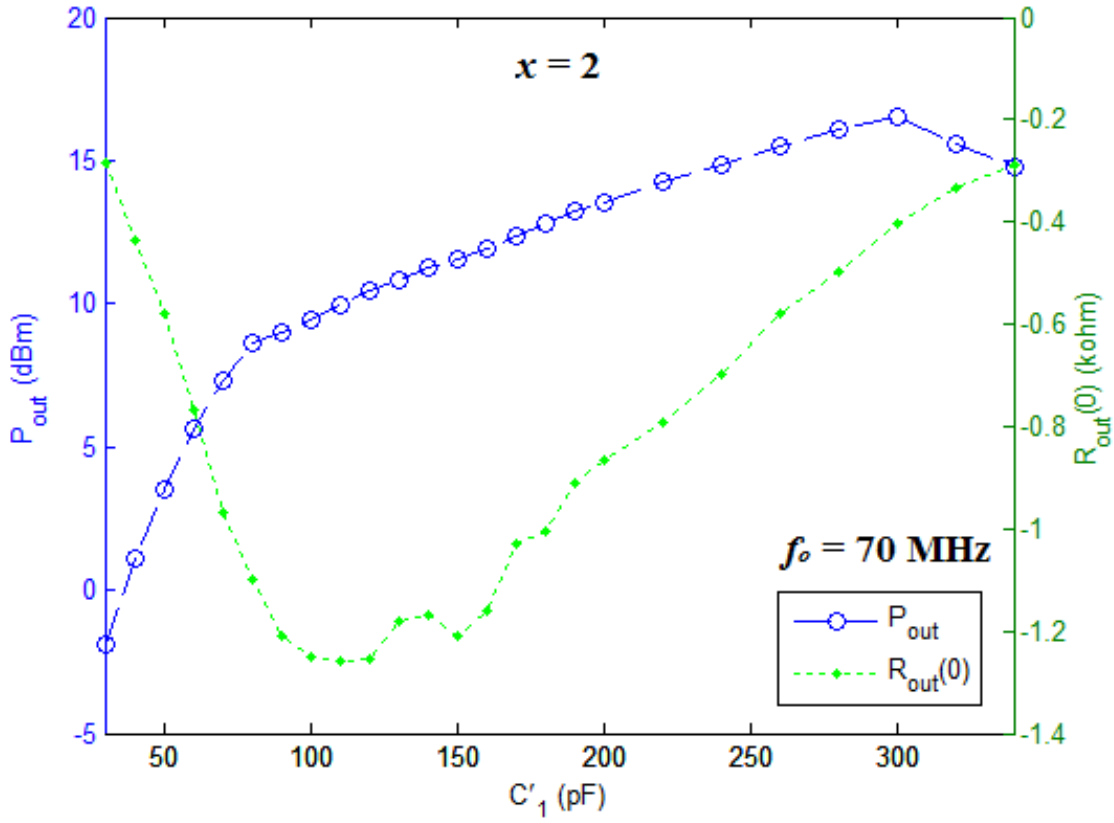

Figure 3.26: Simulation results at 70 MHz. P_{out} (dashed lines) and $R_{out}(0)$ (dotted lines) over a range of C_1' from 30 to 340 pF at $x = 2$. These results are for the series oriented load circuit, where $R_L = \frac{1}{3}R_{out}(0)$.

For the breadboard circuit test, x was set to two as close as possible, and the load was varied for each C_1' value to examine the effect of load variation. The spectrum analyzer input power was measured as in Figure 3.27. With the help of Figure 3.23, the output power was calculated by the following steps:

$$P_{S.A.} = \frac{1}{2} I_L^2 R_{S.A.}, \tag{3.15}$$

Once the spectrum analyzer input power $P_{S.A.}$ is measured, the load (output) current is calculated as follows:

$$\begin{aligned} I_L &= \sqrt{\frac{2P_{S.A.}}{R_{S.A.}}} \\ &= \sqrt{\frac{2P_{S.A.}}{50}}, \end{aligned} \tag{3.16}$$

and the output power is obtained from:

$$\begin{aligned} P_{out} &= \frac{1}{2} I_L^2 R_L \\ &= \frac{1}{2} I_L^2 (R_{ex.} + 50). \end{aligned} \tag{3.17}$$

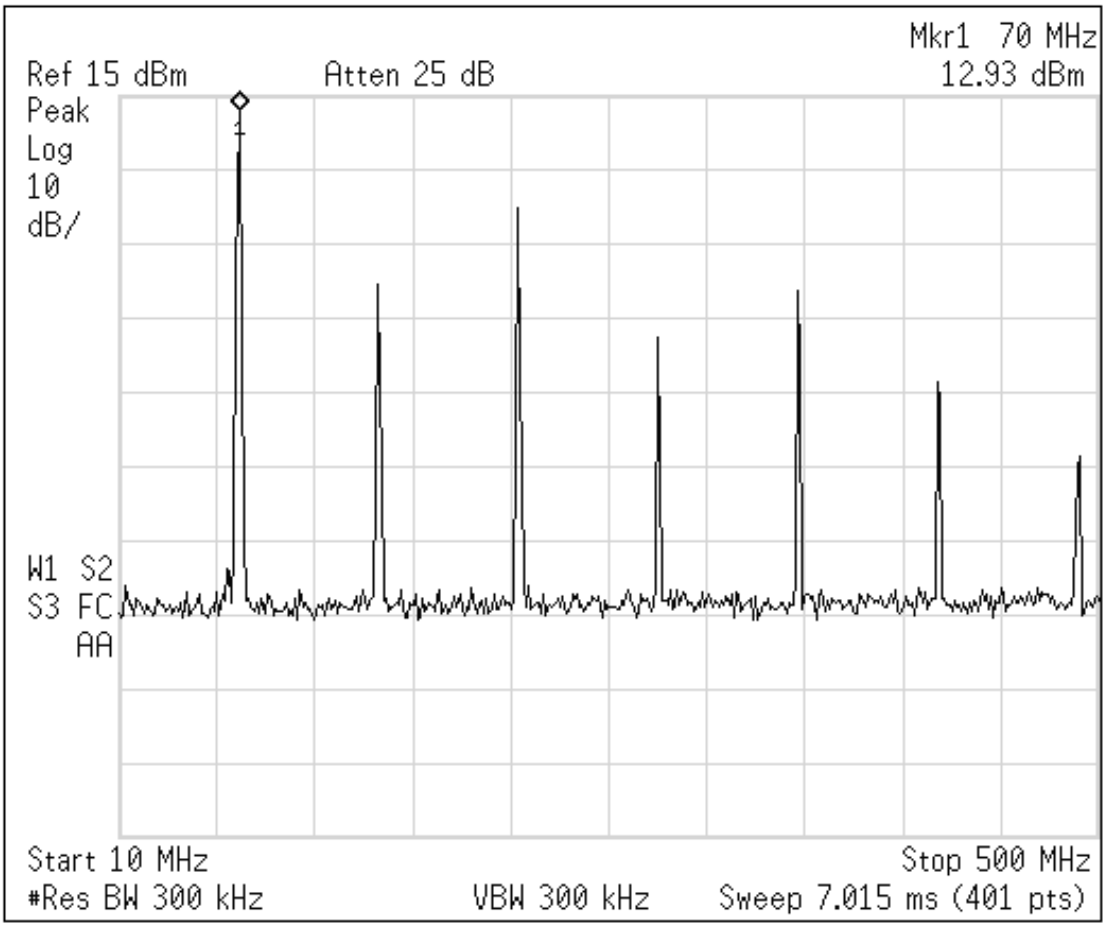

Figure 3.27: Spectrum analyzer screenshot for $P_{S.A}$ with the optimum feedback combination ($C_1' = 64$ pF, $C_2 = 33$ pF and $C_r = 12$ pF). The fundamental and six harmonic components are shown.

The measured output power was plotted against load for different C_1' values, and results are shown in Figure 3.28, where we can see that the power response as a function of load variation is nearly the same for all C_1' values. The highest output powers were delivered for load range of 118 to 201 Ω (for all C_1' values). The maximum output power was 17.1 dBm, and was delivered at $C_1' = 76$ pF and $R_L = 132\ \Omega$. So the highest efficiency was nearly 50%. Measurement results are recorded in “Appendix G”.

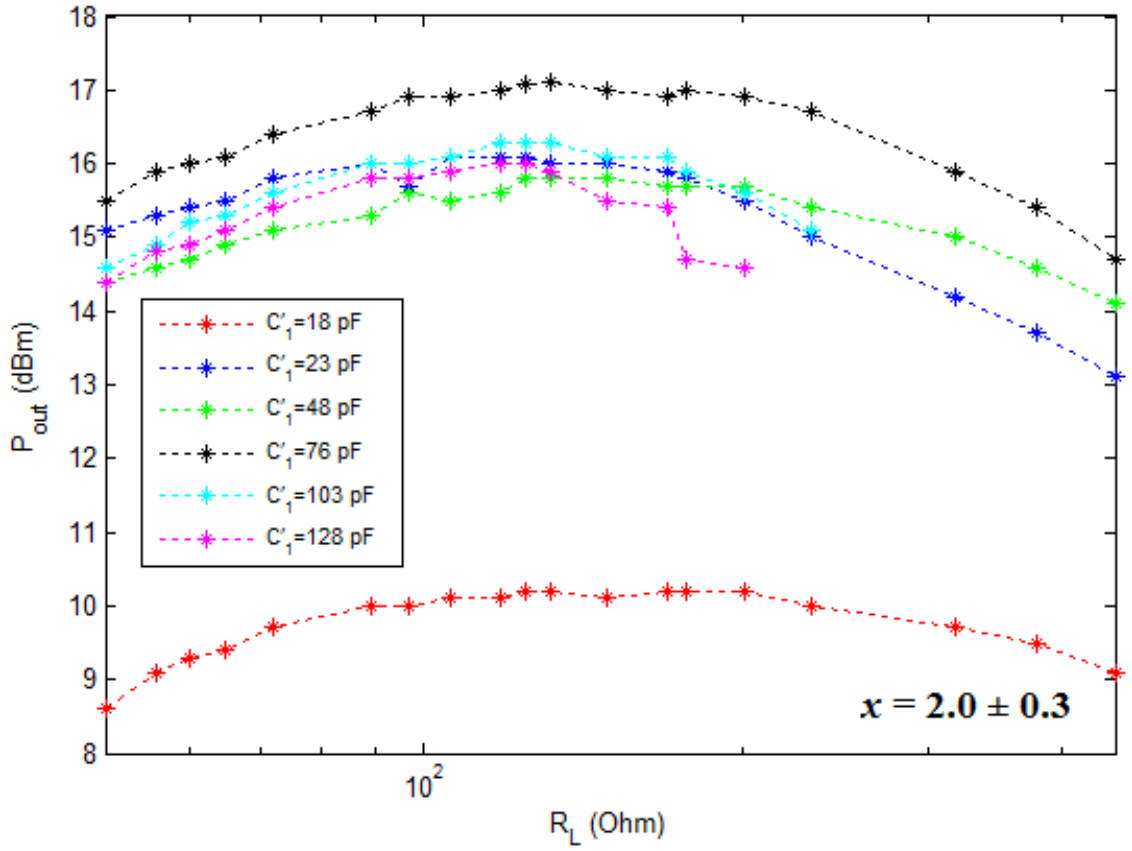

Figure 3.28: Laboratory test results for the output power as a function of load at different C_1' values. The oscillation frequency $f_o = 70$ MHz.

The measured maximum output power was plotted as a function of C_1' in Figure 3.29, and also the corresponding $R_{out}(0)$ was simulated by ADS and plotted in the same graph. From this figure we observe that the maximum output power was delivered at $R_{out}(0) = -1.482$ kΩ, which *is not* the maximum negative resistance. Hence, this practical experiment also confirms the main outcome. Table 3.6 summarizes the main results of this section.

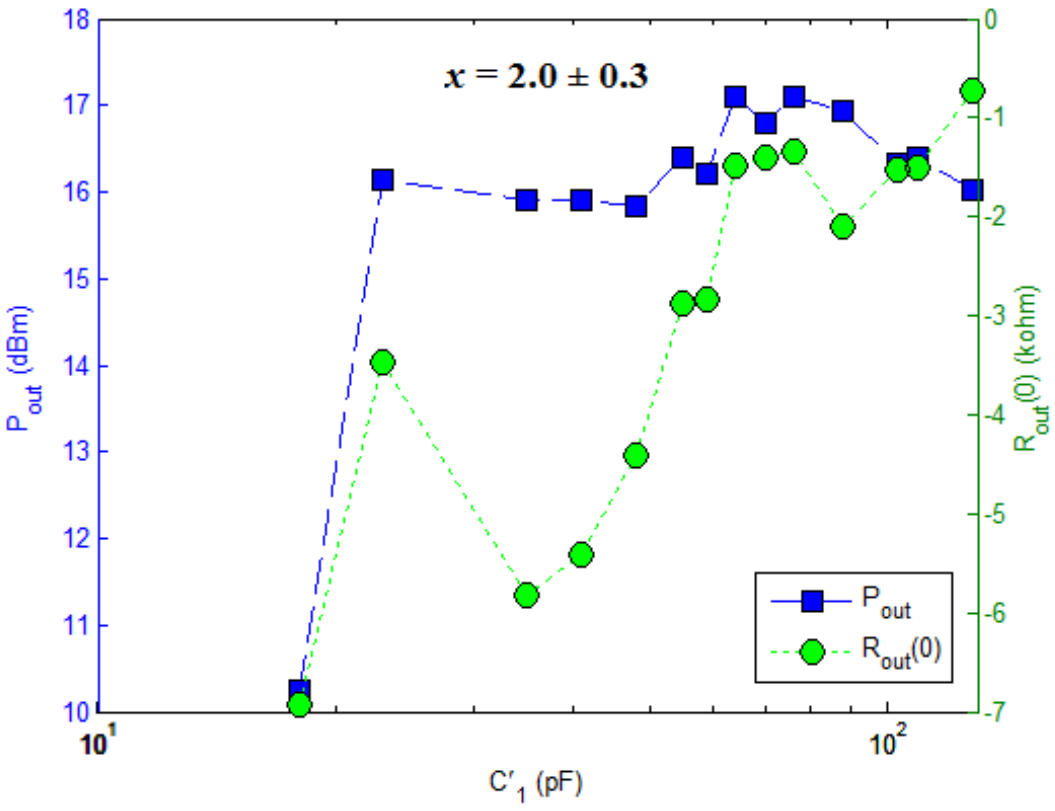

Figure 3.29: Laboratory test results at 70 MHz for the optimum output power as a function of C_1'. The simulated $R_{out}(0)$ curve is also shown.

Table 3.6: Comparison between simulation and laboratory results for the output power of oscillator with series load, at $x = 2$ and $f_o = 70$ MHz.

		$\boldsymbol{P_{out}}$ (dBm)
Simulation results	Maximum P_{out} combination	16.5
	Maximum R_{out} combination	9.9
Laboratory results	Maximum P_{out} combination	17.1
	Maximum R_{out} combination	10.2

4. CONCLUSION

BJT Clapp oscillators with series resonator were designed and analyzed using the negative resistance concept. And they were connected to the load by two possible orientations, parallel and series to the amplifier output port. The feedback elements' reactances were varied while the load was maintained at its supposedly optimal value for maximum output power. The oscillator output power was tested against the negative real part of the small-signal output immittance at startup (i.e, when the oscillation amplitude is nearly zero and begins to rise). The results have shown a significant disapproval with the existing approach that aimed to maximize the output power through maximizing the negative resistance or conductance. In this experiment, the maximum output power was delivered at less than half of the maximum startup negative resistance/conductance. Therefore, results have revealed the deficiency of this approach as one of the current methods for implementing optimum power oscillators. Although this approach was first published in 1975 by Maeda, it is still the basis of state-of-the-art *analytical* methods, as we can learn from Grebennikov's recently published book in 2007 [18].

The design examples revealed also some other interesting results. The load orientation, whether parellel- or series-connected, can make a difference in output power. According to the simulations performed in this thesis, the output power was generally higher to parallel-connected loads than to series-connected loads. Also a difference was observed in optimal coupling capacitances. Capacitances that provided maximum output power were generally lower for the parallel-loads than for the series-loads. This may have some practical implications as what comes to the availability of or preferences for larger or smaller capacitances.

The methods used in this thesis can be applied for other configurations of RF or microwave oscillators to assess the approach under examination. Clearly, further research is recommended to be carried out to invent new methods that can provide more precise basis for maximizing the output power. Some of this research should focus on studying in-depth, analytically or by computer aided design tools, the negative resistance curves in terms of output oscillation amplitude.

REFERENCES

[1] J. K. Clapp. An inductance-capacitance oscillator of unusual frequency stability. Proc. IRE 36(1948)3, pp. 356–358.

[2] M. Maeda, K. Kimura, and H. Kodera. Design and Performance of X-Band Oscillators with GaAs Schottky-Gate Field-Effect Transistors. IEEE Trans. Microw. Theory Tech. 23(1975)8, pp. 661–667. (1975).

[3] D. M. Pozar. Microwave engineering. 4th ed. New Jersey 2011, Wiley. 732 p.

[4] G. Gonzalez. Microwave transistor amplifiers analysis and design. 2nd ed. New Jersey 1996, Prentice-Hall. 506 p.

[5] R. Ludwig and P. Bretchko. RF circuit design theory and applications. New Jersey 2000, Prentice-Hall. 642 p.

[6] R. W. Rhea. Oscillator design and computer simulation. 2nd ed. Georgia 1995, Noble. 320 p.

[7] J. Gewartowski. The effect of series resistance on avalanche diode (IMPATT) oscillator efficiency. Proc. IEEE 56(1968)6, pp. 1139–1140.

[8] A. V. Grebennikov and V. V. Nikiforov. An analytic method of microwave transistor oscillator design. Int. J. Electronics 83(1997)6, pp. 849–858.

[9] A. V. Grebennikov. A simple analytic method for transistor oscillator design. Applied Microwave and Wireless 12(2000)1, pp. 36–44.

[10] A. V. Grebennikov. Microwave transistor oscillators: an analytic approach to simplify computer-aided design. Microwave J. [electronic journal]. (1999), [accessed on 22.03.2013]. Available at: http://www.microwavejournal.com/articles/2640.

[11] O. Lunden, K. Konttinen and M. Hasani. A simple technique for oscillator power calculation. Tampere 2012. To be published.

[12] On Semiconductor. (2013, April 7). MPS918, MPS3563 amplifier transistors data sheet [online]. Available at: http://www.datasheetcatalog.org/datasheet/on_semiconductor/MPS918-D.PDF.

[13] Fairchild Semiconductor. (2013, April 7). PN3563 data sheet [online]. Available at: http://www.foxdelta.com/products/freqcounter/fc3-sk/PN3563.pdf.

[14] J. R. Vig. Quartz crystal resonators and oscillators for frequency control and timing applications- a tutorial. New Jersey 1997, U.S. Army Communications-Electronics Command, SLCET-TR-88-1 (Rev. 8.0). 287 p.

[15] R. Ludwig and G. Bogdanov. RF circuit design theory and applications. 2nd ed. New Jersey 2000, Prentice-Hall. 720 p.

[16] Agilent Technologies. (2013, May 8). ADS 2009 product release [online]. Available at: http://www.home.agilent.com/agilent/product.jspx?nid=-34346.870777.00&lc=eng&cc=GB.

[17] Agilent Technologies. (2013, May 10). E4407B ESA-E Spectrum Analyzer, 9 kHz to 26.5 GHz [online]. Available at: http://www.home.agilent.com/en/pd-1000002791%3Aepsg%3Apro-pn-E4407B/esa-e-spectrum-analyzer-100-hz-to-265-ghz.

[18] A. Grebennikov. RF and microwave transistor oscillator design. Wiley, 2007.

APPENDIX A. SIMULATION RESULTS FOR 100 MHZ CLAPP OSCILLATOR CONNECTED TO PARALLEL LOAD

Table A.1: Simulation results for 100 MHz oscillator with parallel load with $x = 4$ and $(-G_{out}/G_L) = 3.0 \pm 0.1$.

C_1' (pF)	C_r (pF)	L_r (nH)	R_L (Ω)	f_o (MHz)	$G_{out}(0)$ (mS)	$(-G_{out}(0)/G_L)$	P_{out} (dBm)	V_m (V)
15[1]	50	600[2]	373	99.98	-8.04	3.00	14.787	7.109
16	16	600[2]	304	99.7	-9.87	3.00	15.395	6.883
18	33	500	207	100.4	-14.47	3.00	16.396	6.374
20	13	500	162	100.0	-18.49	3.00	17.048	6.078
21	9.7	500	145	100.4	-20.69	3.00	17.369	5.967
22	8.2	500	132	100.5	-22.75	3.00	17.628	5.865
23	7.3	500	120	100.4	-24.9	2.99	17.858	5.742
24	6.6	500	111	100.5	-26.91	2.99	18.006	5.618
25	6.2	500	103	100.2	-29.16	3.00	18.126	5.487
26	5.9	500	95	99.9	-31.51	2.99	18.206	5.318
27	5.7	500	90	99.6	-33.44	3.01	17.991	5.050
28	5.2	500	85	100.4	-35.18	2.99	17.632	4.709
29	5.2	500	81	99.7	-37.26	3.02	17.364	4.457

[1]Combinations for lower C_1' values, in this table and the subsequent tables, with same f_o, x and $-G_{out}/G_L$ values could not be simulated.

[2]Higher L_r values used, in this table and in the subsequent tables, to keep the frequency at 100 MHz approximately.

Table A.2: Simulation results for 100 MHz oscillator with parallel load with $x = 4$ and $(-G_{out}/G_L) = 3.0 \pm 0.1$ (continued).

C_1' (pF)	C_r (pF)	L_r (nH)	R_L (Ω)	f_o (MHz)	$G_{out}(0)$ (mS)	$(-G_{out}(0)/G_L)$	P_{out} (dBm)	V_m (V)
30	5	500	77	99.8	-39.09	3.01	17.043	4.188
35	4.5	500	64	99.5	-47.05	3.01	15.765	3.296
40	4.2	500	57	99.5	-52.92	3.02	14.771	2.774
45	3.9	500	53	100.3	-56.41	2.99	13.927	2.427
50	3.9	500	50	99.5	-59.77	2.99	13.260	2.183
55	3.8	500	49	99.6	-61.29	3.00	12.787	2.047
60	3.7	500	48	99.8	-62.41	3.00	12.304	1.916
65	3.7	500	48	99.5	-62.94	3.02	12.025	1.856
70	3.6	500	48	99.9	-62.98	3.02	11.677	1.783
75	3.6	500	47	99.6	-63.68	2.99	11.284	1.686
80	3.5	500	48	100.1	-62.66	3.01	11.046	1.658
85	3.5	500	48	99.9	-62.93	3.02	10.772	1.606
90	3.5	500	48	99.7	-62.92	3.02	10.498	1.556
95	3.5	500	48	99.5	-62.8	3.01	10.224	1.508
100	3.4	500	48	100.1	-62.37	2.99	9.832	1.442
110	3.4	500	49	99.8	-61.19	3.00	9.361	1.380
120	3.4	500	50	99.6	-60.1	3.01	8.876	1.318
130	3.3	500	51	100.2	-59.26	3.02	8.219	1.234
140	3.3	500	54	100.1	-55.85	3.02	7.824	1.213
150	3.3	500	55	99.9	-54.62	3.00	7.288	1.151
160	3.3	500	57	99.8	-52.92	3.02	6.786	1.106
170	3.3	500	59	99.7	-51.23	3.02	6.261	1.060

Table A.3: Simulation results for 100 MHz oscillator with parallel load with $x = 4$ and $(-G_{out}/G_L) = 3.0 \pm 0.1$ (continued).

C_1' (pF)	C_r (pF)	L_r (nH)	R_L (Ω)	f_o (MHz)	$G_{out}(0)$ (mS)	$(-G_{out}(0)/G_L)$	P_{out} (dBm)	V_m (V)
180	3.3	500	61	99.6	-49.5	3.02	5.714	1.012
190	3.2	500	63	100.3	-47.76	3.01	4.885	0.934
200	3.2	500	69	100.3	-43.78	3.02	4.297	0.914

Table A.4: Simulation results for 100 MHz oscillator with parallel load with $x = 2$ and $(-G_{out}/G_L) = 3.0 \pm 0.1$.

C_1' (pF)	C_r (pF)	L_r (nH)	R_L (Ω)	f_o (MHz)	$G_{out}(0)$ (mS)	$(-G_{out}(0)/G_L)$	P_{out} (dBm)	V_m (V)
10	25	700	677	99.0[3]	-4.55	3.08	12.937	7.740
12	40	570	288	99.8	-10.44	3.01	15.494	6.777
15	14	500	158	100.3	-19	3.00	17.058	6.010
17	8.5	500	121	100.1	-25	3.03	17.808	5.733
19	6.5	500	97	100.3	-30	2.91	18.409	5.501
20	5.9	500	88	100.4	-34	2.99	18.599	5.356
21	5.6	500	83	100.2	-36	2.99	18.649	5.231
22	5.3	500	77	100.1	-39	3.00	18.73	5.086
23	5	500	71	100.3	-42	2.98	18.108	4.546
30	4.2	500	51	100.1	-59	3.01	15.329	2.798
40	3.8	500	38	99.9	-77	2.93	12.815	1.808
50	3.6	500	34	100.0	-87	2.96	11.243	1.427
60	3.5	500	32	99.9	-92	2.94	9.979	1.197
70	3.4	500	31	100.2	-94	2.91	8.894	1.040
80	3.4	500	31	99.8	-96.18	2.98	8.105	0.950
90	3.35	500	31	99.8	-95.83	2.97	7.242	0.860
100	3.3	500	32	100.0	-94	3.01	6.472	0.799
110	3.3	500	33	99.8	-92	3.04	5.749	0.747
120	3.3	500	33	99.6	-90	2.97	4.958	0.682
130	3.2	500	35	100.3	-85	2.98	4.058	0.633

[3]This value exceeds the maximum tolerance.

Table A.5: Simulation results for 100 MHz oscillator with parallel load with $x = 2$ and $(-G_{out}/G_L) = 3.0 \pm 0.1$ (continued).

C_1' (pF)	C_r (pF)	L_r (nH)	R_L (Ω)	f_o (MHz)	$G_{out}(0)$ (mS)	$(-G_{out}(0)/G_L)$	P_{out} (dBm)	V_m (V)
140	3.2	500	38	100.2	-80	3.04	3.294	0.604
150	3.2	500	39	100.0	-77	3.00	2.467	0.557
160	3.2	500	42	99.9	-72	3.02	1.579	0.521
170	3.2	500	45	99.8	-67	3.02	0.617	0.483
180	3.2	500	49	99.7	-61	2.99	-0.464	0.445
190	3.2	500	55	99.6	-54.65	3.01	-1.734	0.408
200	3.1	500	69	100.4	-43.39	2.99	-4.029	0.350

Table A.6: Simulation results for 100 MHz oscillator with parallel load with $x = 1$ and $(-G_{out}/G_L) = 3.0 \pm 0.1$.

C_1' (pF)	C_r (pF)	L_r (nH)	R_L (Ω)	f_o (MHz)	$G_{out}(0)$ (mS)	$(-G_{out}(0)/G_L)$	P_{out} (dBm)	V_m (V)
8	25	720	977	99.9	-3.05	2.98	11.281	7.684
9	20	650	453	100.0	-6.62	3.00	13.896	7.071
10	30	570	281	100.2	-10.67	3.00	15.442	6.654
11	50	500	202	100.5	-14.87	3.00	16.333	6.251
12	18	500	160	99.6	-18.75	3.00	16.965	5.983
13	11	500	132	99.6	-22.79	3.01	17.519	5.792
14	8	500	112	100.2	-26.86	3.01	18.042	5.667
15	6.8	500	97	100.2	-30.9	3.00	18.417	5.506
16	6	500	87	100.5	-34.47	3.00	18.559	5.301
17	5.6	500	77	100.2	-38.45	2.96	18.877	5.173
18	5.3	500	71	99.9	-42.48	3.02	19.069	5.078
19	5	500	65	100.0	-46.45	3.02	19.322	5.002
20	4.8	500	60	99.9	-50.34	3.02	19.534	4.925
22	4.5	500	52	99.8	-57.63	3.00	18.537	4.088
25	4.2	500	44	99.8	-67.39	2.97	16.377	2.932
27	4	500	41	100.1	-73.64	3.02	15.208	2.474
30	3.9	500	37	99.9	-80.77	2.99	13.622	1.958
35	3.7	500	33	100.1	-92.22	3.04	12.152	1.561
40	3.65	500	29	99.7	-102.31	2.97	10.953	1.275
45	3.5	500	28	100.2	-108.78	3.05	10.081	1.133
50	3.4	500	26	100.5	-115.08	2.99	9.008	0.965
55	3.4	500	25	100.1	-121.63	3.04	8.198	0.862

Table A.7: Simulation results for 100 MHz oscillator with parallel load with $x = 1$ and $(-G_{out}/G_L) = 3.0 \pm 0.1$ (continued).

C_1' (pF)	C_r (pF)	L_r (nH)	R_L (Ω)	f_o (MHz)	$G_{out}(0)$ (mS)	$(-G_{out}(0)/G_L)$	P_{out} (dBm)	V_m (V)
60	3.4	500	24	99.8	-123.83	2.97	7.388	0.769
65	3.4	500	24	99.6	-126.74	3.04	6.767	0.716
70	3.3	500	24	100.2	-126.13	3.03	5.971	0.654
75	3.3	500	24	100.0	-127.27	3.05	5.336	0.608
80	3.3	500	24	99.8	-126.83	3.04	4.710	0.565
85	3.3	500	24	99.7	-125.59	3.01	4.102	0.527
90	3.2	500	25	100.4	-122.04	3.05	3.360	0.494
95	3.2	500	25	100.3	-118.98	2.97	2.779	0.462
100	3.2	500	26	100.2	-115.68	3.01	2.208	0.441
110	3.2	500	28	100.0	-107.75	3.02	1.023	0.399
120	3.2	500	31	99.9	-98.34	3.05	-0.273	0.362
130	3.2	500	35	99.7	-86.17	3.02	-1.729	0.325
140	3.2	500	42	99.5	-70.66	2.97	-3.558	0.289
150	3.1	500	74	100.2	-40.37	2.99	-7.76	0.236
160[4]	3.3	480	135	100.2	-22.26	3.01	-13.205	0.170

[4]No output oscillation for C_1' > 160 pF, because $G_{out} > 0$.

Table A.8: Simulation results for 100 MHz oscillator with parallel load with $x = 0.5$ and $(-G_{out}/G_L) = 3.0 \pm 0.1$.

C_1' (pF)	C_r (pF)	L_r (nH)	R_L (Ω)	f_o (MHz)	$G_{out}(0)$ (mS)	$(-G_{out}(0)/G_L)$	P_{out} (dBm)	V_m (V)
8	30	650	507	100.2	-5.92	3.00	13.52	7.163
9	45	560	278	100.5	-10.58	2.94	15.629	6.762
10	40	500	194	100.3	-15.5	3.01	16.663	6.363
11	13	500	147	100.3	-20.42	3.00	17.346	5.992
12	9	500	118	100.1	-25.18	2.98	17.799	5.663
13	7	500	98	100.3	-30.35	2.98	18.325	5.479
14	6	500	84	100.3	-35.77	3.00	18.821	5.368
15	5.4	500	73.6	100.4	-40.75	3.00	19.125	5.204
16	5.2	500	65	99.7	-45.85	2.98	18.564	4.584
17	4.8	500	59	100.1	-50.76	2.99	18.056	4.119
20	4.2	500	46	100.5	-64.72	2.98	17.386	3.367
30	3.7	500	29	99.9	-102.6	2.98	11.323	1.330
40	3.5	500	24	99.8	-127	3.05	7.953	0.821
50	3.3	500	21	100.5	-142	2.98	5.321	0.567
60	3.3	500	21	100.0	-146	3.07	3.273	0.448
70	3.2	500	22	100.4	-138	3.04	1.120	0.358
80	3.2	500	24	100.1	-126	3.02	-0.747	0.302
90	3.2	500	28	99.8	-106.49	2.98	-2.798	0.257
100	3.1	500	49	100.4	-61.34	3.01	-7.055	0.208
105[5]	3.1	500	62	100.3	-48.74	3.02	-9.430	0.178

[5]No output oscillation for C_1' > 105 pF, because $G_{out} > 0$.

Table A.9: Simulation results for 100 MHz oscillator with parallel load with $x = 0.25$ and $(-G_{out}/G_L) = 3.0 \pm 0.1$.

C_1' (pF)	C_r (pF)	L_r (nH)	R_L (Ω)	f_o (MHz)	$G_{out}(0)$ (mS)	$(-G_{out}(0)/G_L)$	P_{out} (dBm)	V_m (V)
8	70	570	315	100.5	-9.53	3.00	15.372	6.988
9	15	540	201	100.5	-14.96	3.01	14.401	4.992
10	12	510	147	100.1	-20.23	2.97	16.117	5.201
11	8.9	500	114	99.7	-26.18	2.98	16.836	4.976
12	6.8	500	93	100.0	-32.31	3.00	16.729	4.439
13	5.8	500	78	100.1	-38.31	2.99	16.229	3.838
14	5.2	500	68	100.2	-44.43	3.02	15.543	3.311
15	4.9	500	59	99.9	-50.45	2.98	15.143	2.946
20	4.1	500	38	99.6	-78.93	3.00	13.567	1.972
25	3.7	500	29	100.1	-102.68	2.98	9.337	1.058
30	3.5	500	25	100.4	-121.11	3.03	6.187	0.684
35	3.4	500	22	100.4	-135.15	2.97	4.241	0.513
40	3.4	500	21	99.8	-145.71	3.06	2.552	0.412
45	3.3	500	20	100.2	-147.05	2.941	0.759	0.327
50	3.3	500	21	99.8	-144.3	3.03	-0.791	0.281
55	3.2	500	23	100.4	-130.99	3.01	-2.581	0.239
60	3.2	500	27	100.1	-110.68	2.99	-4.372	0.211
65	3.2	500	34	99.9	-89.08	3.03	-6.584	0.183
70[6]	3.2	500	56	99.6	-53.63	3.00	-10.486	0.150

[6]No output oscillation for C_1' > 70 pF, because $G_{out} > 0$.

APPENDIX B. SIMULATION RESULTS FOR 100 MHZ CLAPP OSCILLATOR CONNECTED TO SERIES LOAD

Table B.1: Simulation results for 100 MHz oscillator with series load with $x = 4$ and $(-R_{out}/R_L) = 3.0 \pm 0.1$.

C_1' (pF)	C_r (pF)	L_r (nH)	R_L (Ω)	f_o (MHz)	$R_{out}(0)$ (Ω)	$(-R_{out}(0)/R_L)$	P_{out} (dBm)	I_m (mA)
15	20	500	3100	99.8	-9445	3.05	3.018	1.7
20	8	500	2918	99.8	-8987	3.08	4.302	2.0
30	5	500	2066	100.2	-6202	3.00	6.212	3.0
40	4.3	500	1534	100.0	-4543	2.96	7.534	4.1
50	4	500	1195	99.8	-3530	2.95	8.492	5.2
60	3.8	500	951	99.8	-2807	2.95	9.341	6.4
70	3.7	500	781	99.6	-2301	2.95	10.066	7.6
80	3.5	500	615	100.4	-1827	2.97	10.884	9.5
90	3.55	500	535	99.6	-1590	2.97	11.381	10.8
100	3.5	500	448	99.6	-1337	2.98	11.984	12.6
110	3.4	500	367	100.0	-1097	2.99	12.661	15.0
120	3.4	500	314	99.7	-943	3.00	13.183	17.3
130	3.4	500	270	99.5	-811	3.00	13.698	19.8
140	3.3	500	220	100.1	-662	3.01	14.390	23.7
150	3.3	500	190	99.9	-570	3.00	14.877	27.0

Table B.2: Simulation results for 100 MHz oscillator with series load with $x = 4$ and $(-R_{out}/R_L) = 3.0 \pm 0.1$ (continued).

C_1' (pF)	C_r (pF)	L_r (nH)	R_L (Ω)	f_o (MHz)	$R_{out}(0)$ (Ω)	$(-R_{out}(0)/R_L)$	P_{out} (dBm)	I_m (mA)
160	3.3	500	164	99.7	-491	2.99	15.337	30.6
165	3.3	500	152	99.6	-456	3.00	15.558	32.6
168	3.3	500	145	99.6	-436	3.01	15.687	33.9
170	3.3	500	141	99.6	-423	3.00	15.77	34.7
171	3.2	500	130	100.4	-389	2.99	15.992	37.1
172	3.2	500	128	100.4	-383	2.99	16.028	37.5
173	3.2	500	126	100.4	-377	2.99	16.060	38.0
174	3.2	500	124	100.4	-371	2.99	16.087	38.4
175	3.2	500	122	100.4	-365	2.99	16.104	38.8
176	3.2	500	120	100.3	-359	2.99	16.101	39.1
177	3.2	500	118	100.3	-354	3.00	16.061	39.2
178	3.2	500	116	100.3	-349	3.01	15.993	39.3
179	3.2	500	115	100.3	-344	2.99	15.937	39.2
180	3.2	500	113	100.3	-338	2.99	15.860	39.2
181	3.2	500	111	100.3	-333	3.00	15.781	39.2
182	3.2	500	109	100.3	-328	3.01	15.701	39.2
183	3.2	500	108	100.3	-323	2.99	15.642	39.1
184	3.2	500	106	100.3	-317	2.99	15.559	39.1
185	3.2	500	104	100.2	-313	3.01	15.475	39.1
190	3.2	500	96	100.2	-289	3.01	15.089	38.9
200	3.2	500	82	100.1	-247	3.01	14.306	38.5

Table B.3: Simulation results for 100 MHz oscillator with series load with $x = 2$ and $(-R_{out}/R_L) = 3.0 \pm 0.1$.

C_1' (pF)	C_r (pF)	L_r (nH)	R_L (Ω)	f_o (MHz)	$R_{out}(0)$ (Ω)	$(-R_{out}(0)/R_L)$	P_{out} (dBm)	I_m (mA)
30	4.2	500	436	100.0	-1178	2.70[6]	8.916	9.0
35	4	500	422	99.9	-1230	2.91	9.206	9.4
40	3.8	500	448	100.1	-1343	3.00	9.579	9.5
45	3.7	500	483	99.9	-1460	3.02	10.175	9.8
50	3.6	500	476	100.0	-1437	3.02	10.806	10.7
55	3.5	500	430	100.3	-1291	3.00	11.395	12.0
60	3.5	500	404	99.9	-1234	3.05	11.842	13.0
70	3.4	500	336	100.1	-1008	3.00	12.826	16.0
80	3.4	500	290	99.6	-881	3.04	13.529	18.7
90	3.3	500	232	100.1	-695	3.00	14.370	23.0
100	3.3	500	197	99.8	-597	3.03	15.043	27.0
110	3.3	500	161	99.5	-499	3.10	15.736	32.4
120	3.2	500	128	100.1	-394	3.08	16.473	39.5
121	3.2	500	128	100.1	-385	3.01	16.499	39.6
122	3.2	500	126	100.1	-377	2.99	16.530	40.1
123	3.2	500	123	100.1	-368	2.99	16.544	40.6
124	3.2	500	120	100.1	-359	2.99	16.494	40.9
125	3.2	500	119	100.0	-358	3.01	16.414	40.7
130	3.2	500	106	100.0	-321	3.03	15.833	40.3
140	3.2	500	85	99.9	-260	3.06	14.631	39.2

[6]This value exceeds the maximum tolerance.

Table B.4: Simulation results for 100 MHz oscillator with series load with $x = 2$ and $(-R_{out}/R_L) = 3.0 \pm 0.1$ (continued).

C_1' (pF)	C_r (pF)	L_r (nH)	R_L (Ω)	f_o (MHz)	$R_{out}(0)$ (Ω)	$(-R_{out}(0)/R_L)$	P_{out} (dBm)	I_m (mA)
150	3.2	500	68	99.8	-208	3.06	13.396	38.0
160	3.2	500	54	99.7	-166	3.07	12.121	36.9
170	3.1	500	37	100.5	-112	3.03	10.011	34.9
170	3.1	500	37	100.5	-112	3.03	10.011	34.9
180	3.1	500	28	100.4	-84	3.00	8.357	33.2
190	3.1	500	20	100.3	-59	2.95	6.276	30.9
200	3.1	500	12.67	100.2	-38	3.00	3.428	28.0

Table B.5: Simulation results for 100 MHz oscillator with series load with $x = 1$ and $(-R_{out}/R_L) = 3.0 \pm 0.1$.

C_1' (pF)	C_r (pF)	L_r (nH)	R_L (Ω)	f_o (MHz)	$R_{out}(0)$ (Ω)	$(-R_{out}(0)/R_L)$	P_{out} (dBm)	I_m (mA)
35	3.7	500	37	100.1	-111	3.00	11.812	43.0
40	3.6	500	70	99.9	-205	2.93	13.039	36.0
45	3.5	500	97	100.0	-290	2.99	13.367	31.7
50	3.4	500	127	100.2	-382	3.01	14.016	29.9
60	3.4	500	121	99.6	-363	3.00	14.993	34.3
70	3.3	500	125	99.8	-384	3.07	15.979	37.8
75	3.3	500	121	99.6	-370	3.06	16.338	40.0
79	3.2	500	112	100.3	-336	3.00	16.708	43.4
80	3.2	500	107	100.3	-321	3.00	16.756	44.6
81	3.2	500	111	100.2	-333	3.00	16.747	43.8
82	3.2	500	107	100.2	-320	2.99	16.645	44.1
90	3.2	500	90	100.0	-274	3.04	16.441	46.9
100	3.2	500	68	99.8	-210	3.09	13.679	39.3
110	3.2	500	51	99.7	-157	3.08	11.843	36.7
120	3.1	500	35	100.4	-104	2.97	9.384	33.4
130	3.1	500	22.61	100.3	-67.82	3.00	6.664	30.4
140	3.1	500	12.66	100.2	-37.98	3.00	2.744	25.9
150[7]	3.1	500	4.38	100.1	-13.14	3.00	-4723	18.6

[7]No output oscillation for C_1' > 150 pF, because $R_{out} > 0$.

Table B.6: Simulation results for 100 MHz oscillator with series load with $x = 0.5$ and $(-R_{out}/R_L) = 3.0 \pm 0.1$.

C_1' (pF)	C_r (pF)	L_r (nH)	R_L (Ω)	f_o (MHz)	$R_{out}(0)$ (Ω)	$(-R_{out}(0)/R_L)$	P_{out} (dBm)	I_m (mA)
40	3.4	500	14	100.3	-41	2.93	12.915	79.3
42	3.4	500	17	100.1	-51	3.00	14.063	82.1
44	3.4	500	23.3	99.9	-70	3.00	15.104	79.1
45	3.4	500	25.2	99.8	-75.7	3.00	15.111	76.1
46	3.4	500	26.3	99.7	-79	3.00	14.933	73.0
47	3.4	500	27	99.6	-80.77	2.99	14.672	69.9
50	3.3	500	34	100.2	-101	2.97	14.036	57.9
55	3.3	500	35	99.9	-102.08	2.92	13.187	51.8
60	3.2	500	45.88	100.4	-137.63	3.00	13.298	45.8
65	3.2	500	43	100.2	-129	3.00	12.192	41.6
70	3.2	500	43	100.0	-128	2.98	11.57	38.8
75	3.2	500	36	99.9	-109	3.03	10.248	36.4
80	3.2	500	30	99.7	-89	2.97	8.895	34.1
85	3.2	500	24	99.6	-72	3.00	7.345	31.9
90	3.1	500	17	100.4	-50	2.94	4.774	28.2
95	3.1	500	11.48	100.3	-34.44	3.00	1.874	24.6
100	3.1	500	6.68	100.2	-20.03	3.00	-2.393	19.7
105[8]	3.1	500	2.11	100.1	-6.32	3.00	-11.768	11.9

[8]No output oscillation for C_1' > 105 pF, because $R_{out} > 0$.

Table B.7: Simulation results for 70 MHz oscillator with series load with $x = 2$ and $(-R_{out}/R_L) = 3.00 \pm 0.01$.

C_1' (pF)	C_r (pF)	L_r (nH)	R_L (Ω)	f_o (MHz)	$R_{out}(0)$ (Ω)	$(-R_{out}(0)/R_L)$	P_{out} (dBm)
30	45	500	95	71.0	-285	3.00	-1.861
40	22	500	145	70.3	-435	3.00	1.097
50	16	500	193	70.6	-580	3.01	3.510
60	13.5	500	256	70.8	-768	3.00	5.642
70	12.5	500	323	70.4	-968	3.00	7.317
80	11.5	500	367	70.7	-1101	3.00	8.597
90	11	500	403	70.6	-1209	3.00	9.019
100	10.6	500	417	70.6	-1250	3.00	9.412
110	10.2	500	420	70.8	-1259	3.00	9.939
120	10	500	418	70.7	-1255	3.00	10.440
130	10	500	393	70.3	-1179	3.00	10.859
140	10	500	389	69.9	-1167	3.00	11.244
150	10	500	403	69.5	-1209	3.00	11.586
160	10	500	386	69.2	-1159	3.00	11.947
170	10	500	343	69.0	-1028	3.00	12.345
180	9.8	500	334	69.2	-1003	3.00	12.770
190	9.6	500	304	69.5	-912	3.00	13.239
200	9.6	500	289	69.3	-867	3.00	13.562
220	9.4	500	265	69.4	-794	3.00	14.259
240	9.4	500	233	69.1	-699	3.00	14.853
260	9.2	500	194	69.4	-581	2.99	15.539

Table B.8: Simulation results for 70 MHz oscillator with series load with $x = 2$ and $(-R_{out}/R_L) = 3.00 \pm 0.01$ (continued).

C_1' (pF)	C_r (pF)	L_r (nH)	R_L (Ω)	f_o (MHz)	$R_{out}(0)$ (Ω)	$(-R_{out}(0)/R_L)$	P_{out} (dBm)
280	9.2	500	166	69.2	-498	3.00	16.073
300	9	500	134	69.6	-402	3.00	16.530
320	9	500	111	69.5	-332	2.99	15.593
340	9	500	96	69.3	-288	3.00	14.747

APPENDIX C. G-V GRAPHS FOR THE OSCILLATOR WITH PARALLEL LOAD

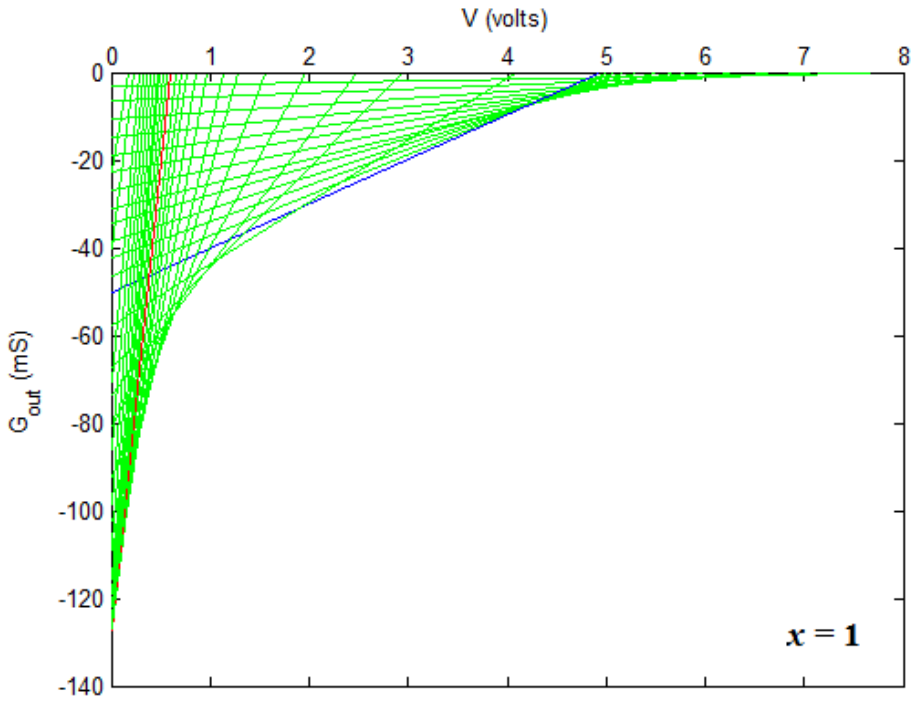

Figure C.1: Simulation results for the small-signal output conductance G_{out} as a function of V with $x = 1$. a) Blue line: maximum power combination. b) Red line: maximum conductance combination. c) Green lines: other combinations.

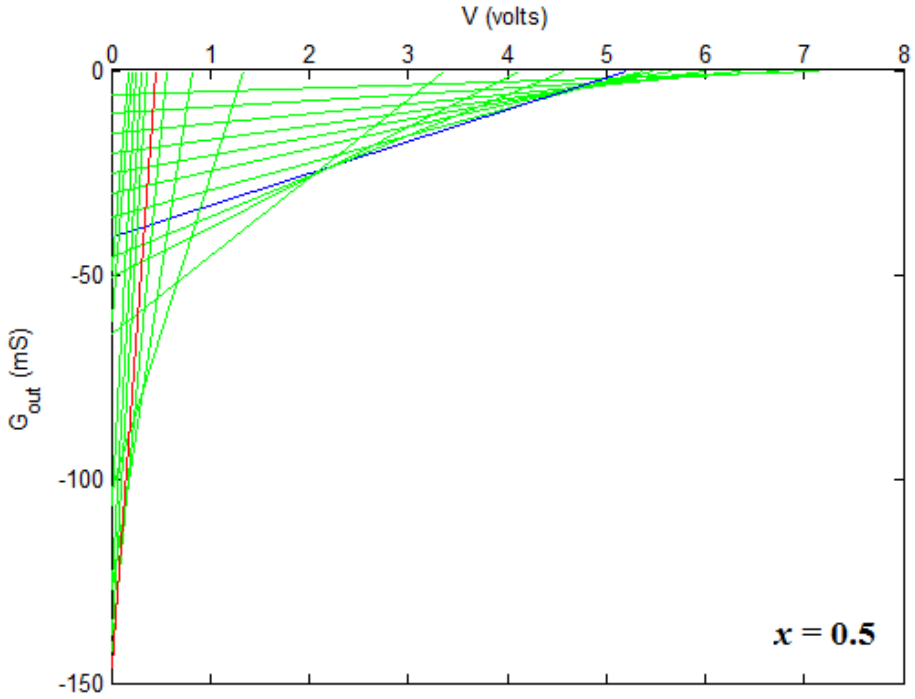

Figure C.2: Simulation results for the small-signal output conductance G_{out} as a function of V with $x = 0.5$. a) Blue line: maximum power combination. b) Red line: maximum conductance combination. c) Green lines: other combinations.

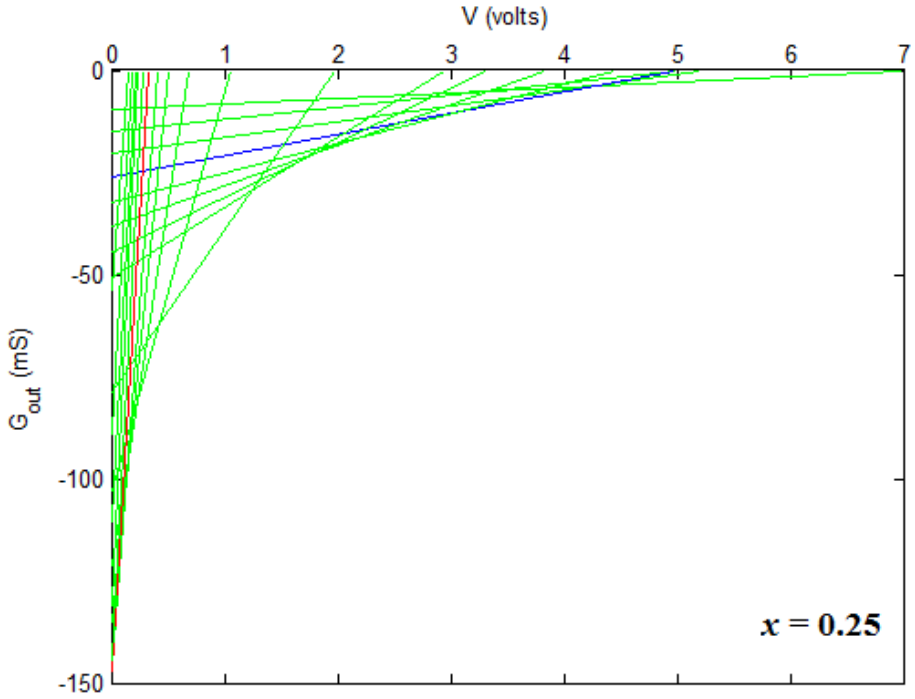

Figure C.3: Simulation results for the small-signal output conductance G_{out} as a function of V with $x = 0.25$. a) Blue line: maximum power combination. b) Red line: maximum conductance combination. c) Green lines: other combinations.

APPENDIX D. R-I GRAPHS FOR THE OSCILLATOR WITH SERIES LOAD

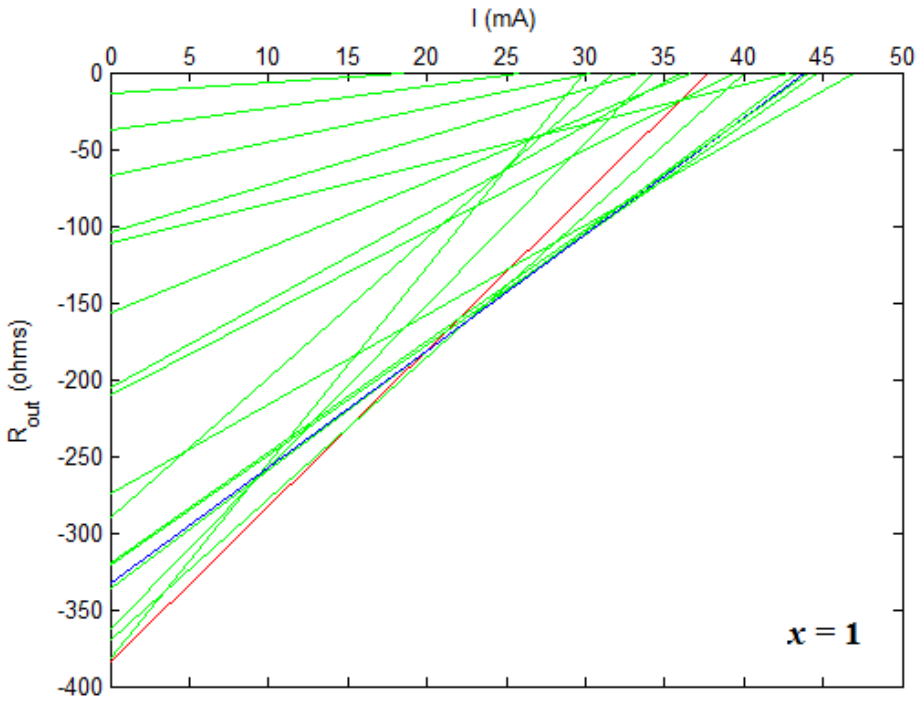

Figure D.1: Simulation results for the small-signal output resistance R_{out} as a function of I with $x = 1$. a) Blue line: maximum power combination. b) Red line: maximum resistance combination. c) Green lines: other combinations.

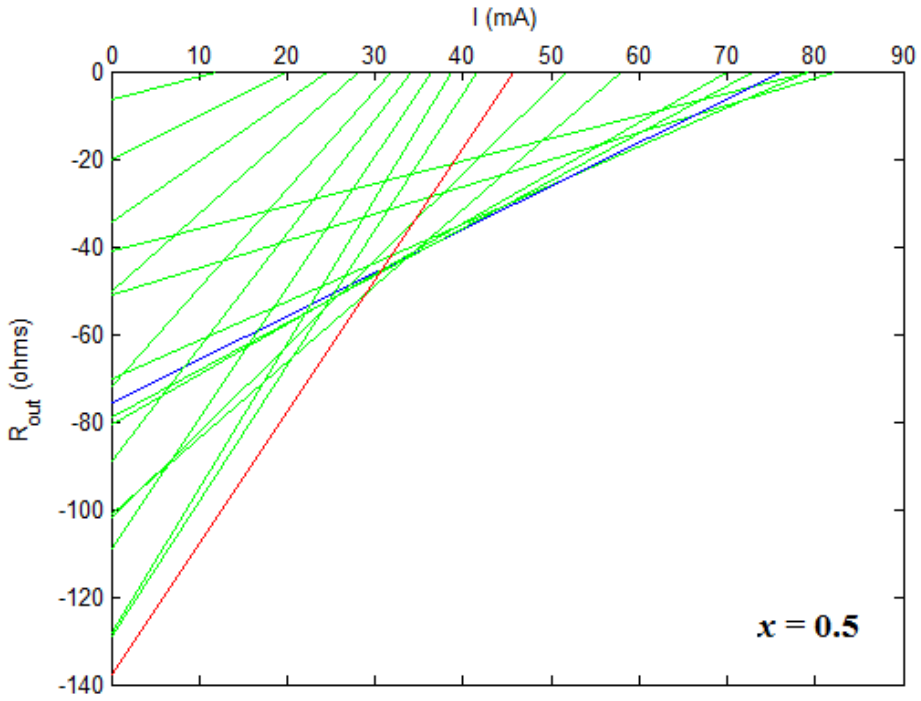

Figure D.2: Simulation results for the small-signal output resistance R_{out} as a function of I with $x = 0.5$. a) Blue line: maximum power combination. b) Red line: maximum resistance combination. c) Green lines: other combinations.

APPENDIX E. RESONATOR INDUCTOR CALCULATION

The goal here is to design a 500-nH air-wound coil with a high quality factor. The coil is made from a copper wire with a diameter $d = 0.8$ mm. For a high quality factor, the space between adjacent turns s was chosen such that space-to-diameter ratio (s/d) is equal to 1.5. To calculate the number of turns needed, the following formula was used:

$$L_r = \frac{B^2 N^2}{0.45B + A} \qquad \text{For } A \geq 0.4B, \tag{E.1}$$

where B is the coil diameter in millimeters, A is the coil length in millimeters and N is the number of turns.

The coil length A in terms of the number of turns was expressed as:

$$\begin{aligned} A &= Ns \\ &= N(1.5d) \\ &= N(1.5)(0.8) \\ &= 1.2N, \end{aligned} \tag{E.2}$$

and the coil diameter B was chosen to be 10 mm. By substituting coil parameters (A and B) in equation (E.1), the number of turns can be calculated as follows:

$$L_r = \frac{10^2 N^2}{(0.45)(10) + 1.2N}, \tag{E.3}$$

$$100N^2 - 600N - 2250 = 0, \tag{E.4}$$

$$N = \begin{cases} 8.6 \\ \text{or} \\ -2.6 \text{ (rejected)}, \end{cases} \tag{E.5}$$

$$N = 8.6 \approx 9 \text{ turns}. \tag{E.6}$$

To verify the condition mentioned in equation (E.1), we calculated A and found that

$$A = 1.2N = (1.2)(8.6) = 10.32 \text{ mm}, \tag{E.7}$$

(note that A is approximatly equal to B, and that gives a higher quality factor)

$$0.4B = (0.4)(10) = 4 \text{ mm}. \tag{E.8}$$

From equations (E.7) and (E.8):

$$A > 0.4B. \tag{E.9}$$

Practically, a 500-nH inductor was designed using eight turns only. The final specifications of the designed resonator inductor are shown in Table E.1.

Table E.1: Resonator inductor specifications.

Parameter	**Value**
Wire diameter (d)	0.8 mm
Space between turns (s)	1.2 mm
Coil length (A)	9.6 mm
Coil diameter (B)	10 mm
Number of turns (N)	8 turns
space to distance ratio (s/d)	1.5

APPENDIX F. TRANSISTOR BIASING

The aim here is to bias the transistor used to achieve an operating point $V_{CEQ} = 5$ V and $I_{CQ} = 20$ mA using two resistor biasing circuit, and to know the value of the current that should be drawn from the DC source I_{CC}.

For the oscillator connected to parallel load

The current gain (β) was unknown at the beginning, so a transient simulation was run several times for the circuit shown in Figure F.1. The DC source voltage (V_{CC}) was fixed at 5 volts, while the two biasing resistors R_1 and R_2 were varied to achieve the desired quiescent point ($V_{CEQ} = 5$ V, $I_{CQ} = 20$ mA). The final biasing settings are extracted from Figure F.1 and summarized in Table F.1.

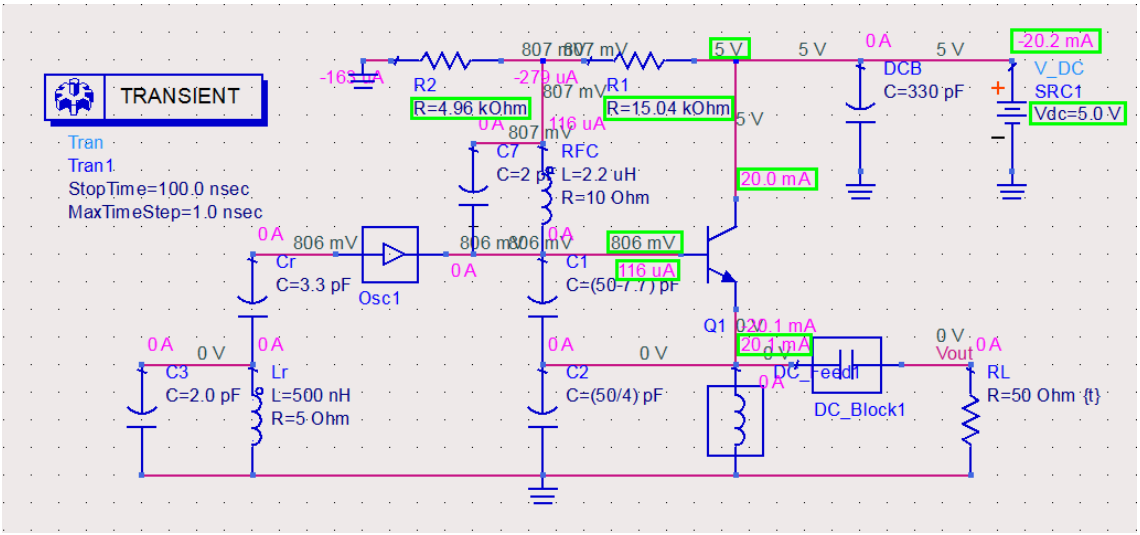

Figure F.1: Clapp Oscillator schematic with DC annotations, where the load is connected in parallel.

Table F.1: Transistor biasing settings for the oscillator with parallel load.

V_{CEQ}	I_{CQ}	V_{CC}	I_{CC}	R_1	R_2	V_{BE}	I_B	β
5	20	5	20.2	15.04	4.96	0.806	116	172.4
V	**mA**	**V**	**mA**	**kΩ**	**kΩ**	**V**	**μA**	

If β were precisely known, then the following mathematical solution would have been carried out. We assume the biasing equivalent circuit shown in Figure F.2, where all RF chokes and DC blocks are ideal. Applying KCL at node (1):

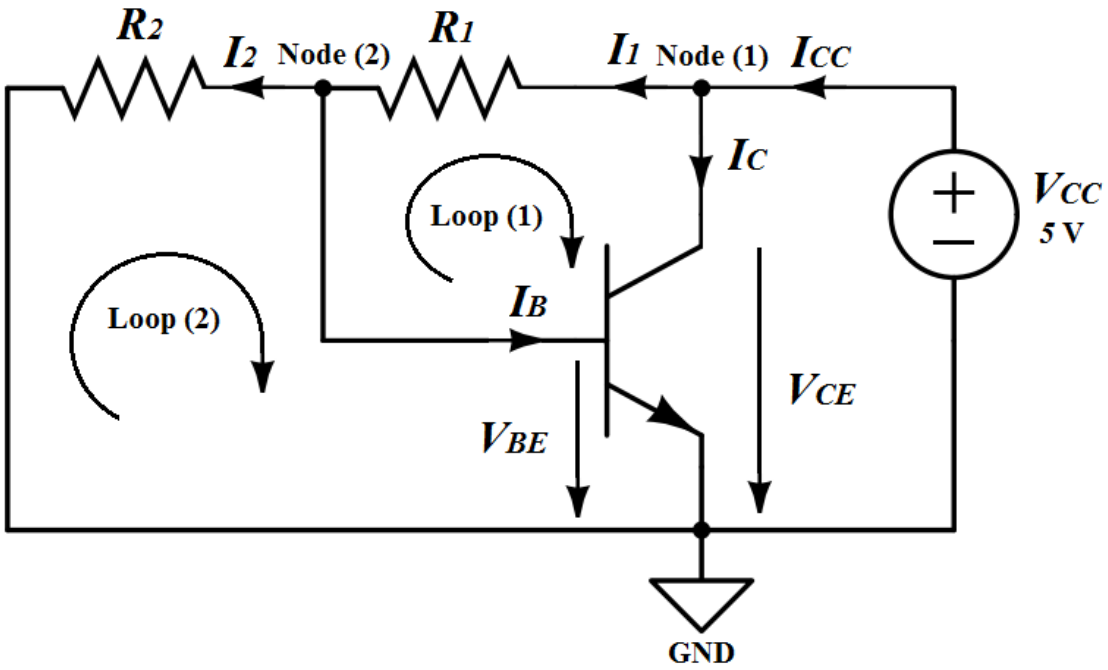

Figure F.2: Transistor equivalent biasing circuit.

$$I_{CC} = I_1 + I_C. \tag{F.1}$$

Applying KCL at node (2):

$$I_1 = I_2 + I_B. \tag{F.2}$$

Substituting equation (F.2) in equation (F.1) :

$$\begin{aligned} I_{CC} &= I_2 + I_B + I_C \\ &= I_2 + \frac{I_C}{\beta} + I_C \\ &= I_2 + (1 + \frac{1}{\beta})I_C. \end{aligned} \tag{F.3}$$

Considering $\beta = 172.4$:

$$I_{CC} = I_2 + (1 + \frac{1}{172.4})(0.02) = (I_2 + 0.0201)\ \text{A}. \tag{F.4}$$

Applying KVL at loop (1):

$$\begin{aligned} V_{CE} &= V_{BE} + I_1 R_1 \\ &= V_{BE} + (I_2 + I_B) R_1 \\ &= V_{BE} + (I_2 + \frac{I_C}{\beta}) R_1 \end{aligned} \tag{F.5}$$

$$5 = 0.806 + (I_2 + \frac{(20)(10^{-3})}{172.4}) R_1, \tag{F.6}$$

$$I_2 R_1 + (1.16)(10^{-4}) R_1 - 4.194 = 0. \tag{F.7}$$

Applying KVL at loop (2):

$$\begin{aligned} V_{BE} &= R_2 I_2 \\ &= (20000 - R_1) I_2 \end{aligned} \tag{F.8}$$

$$0.806 = (20000 - R_1) I_2, \tag{F.9}$$

$$20000 I_2 - I_2 R_1 - 0.806 = 0. \tag{F.10}$$

Solving equation (F.7) and (F.10) together by Matlab to find I_2 and R_1:

$$(I_2, R_1) = \begin{cases} 160\ \mu\text{A},\ 15.047\ \text{k}\Omega \\ \text{or} \\ -28\ \mu\text{A},\ 48.056\ \text{k}\Omega\ \text{(rejected because } R_1 > 20\ \text{k}\Omega\text{)}. \end{cases} \tag{F.11}$$

Substituting $I_2 = 160\ \mu$A in equation (F.4) to find I_{CC}:

$$\begin{aligned} I_{CC} &= I_2 + 0.0201 \\ &= (160)(10^{-6}) + 0.02012 = 20.28\ \text{mA}, \end{aligned} \tag{F.12}$$

$$\begin{aligned} R_2 &= 20000 - R_1 \\ &= 20000 - 15047 = 4.953\ \text{k}\Omega. \end{aligned} \tag{F.13}$$

The final results for I_{CC}, R_1 and R_2 are similar to what are obtained by simulation.

For the oscillator connected to series load

The DC source voltage was set to 5.2 volts to compensate the RF choke voltage drop, as shown in Figure F.3. A transient simulations were done with varying R_1 and R_2 to obtain the same desired quiescent point. The final biasing settings are shown in Table F.2.

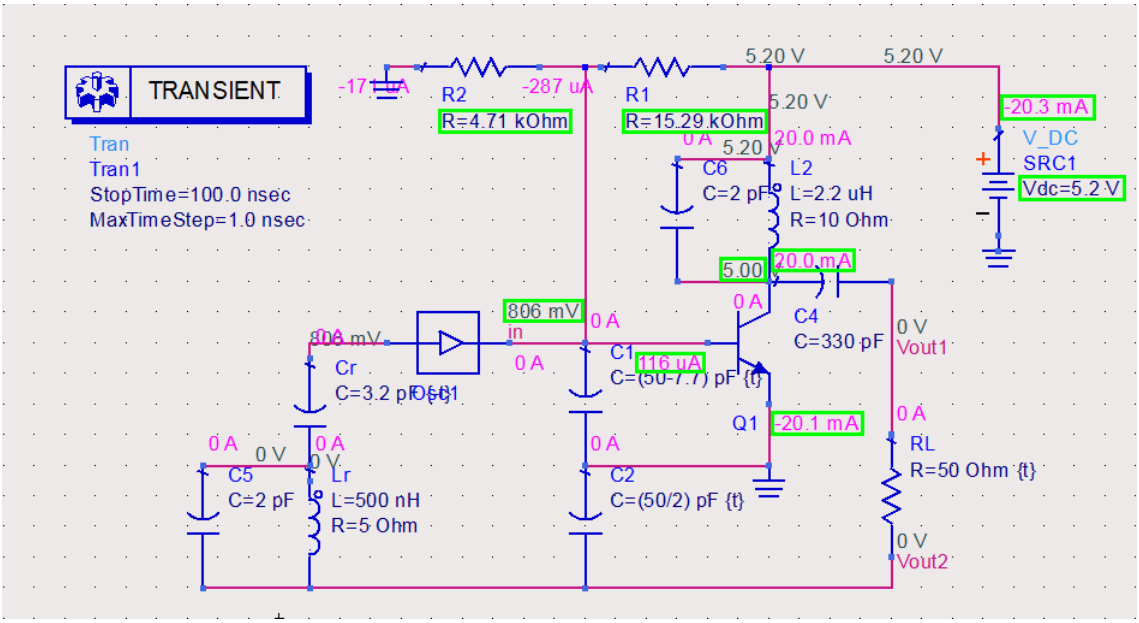

Figure F.3: Clapp Oscillator schematic with DC annotations, where the load is connected in series.

Table F.2: Transistor biasing settings for the oscillator with series load.

V_{CEQ}	I_{CQ}	V_{CC}	I_{CC}	R_1	R_2	V_{BE}	I_B	β
5	20	5.2	20.3	15.29	4.71	0.806	116	172.4
V	**mA**	**V**	**mA**	**kΩ**	**kΩ**	**V**	**μA**	

APPENDIX G. LABORATORY MEASUREMENTS FOR THE OSCILLATOR WITH SERIES LOAD

Table G.1: Spectrum analyzer input power against $R_{ex.}$ for $C_1' = 18$, 23, 35, 41 and 48 pF, $x = 2.0 \pm 0.3$.

$R_{ex.}(\Omega)$	$P_{S.A}$ (dBm)				
	$C_1' = 18$ pF $C_2 = 10$ pF $C_r = 15$ pF	$C_1' = 23$ pF $C_2 = 10$ pF $C_r = 12$ pF	$C_1' = 35$ pF $C_2 = 18$ pF $C_r = 12$ pF	$C_1' = 41$ pF $C_2 = 18$ pF $C_r = 12$ pF	$C_1' = 48$ pF $C_2 = 22$ pF $C_r = 12$ pF
0	8.6	15.1	14.2	14.3	14.4
6	8.6	14.8	14.0	14.0	14.1
10	8.5	14.6	13.6	13.9	13.9
15	8.3	14.4	13.6	13.7	13.8
22	8.1	14.2	13.3	13.5	13.5
39	7.5	13.5	12.6	12.9	12.8
47	7.1	12.8	12.6	12.8	12.7
56	6.8	12.8	12.2	12.4	12.2
68	6.4	12.4	12.0	12.1	11.9
75	6.2	12.1	11.9	11.9	11.8
82	6.0	11.8	11.6	11.6	11.6
99	5.4	11.3	11.0	11.1	11.1
120	4.9	10.6	10.4	10.5	10.4
127	4.7	10.3	10.2	10.3	10.2

Table G.2: Spectrum analyzer input power against $R_{ex.}$ for $C_1' = 18$, 23, 35, 41 and 48 pF, $x = 2.0 \pm 0.3$ (continued).

$\boldsymbol{R_{ex.}(\Omega)}$	$\boldsymbol{P_{S.A}}$ (dBm)				
	$\boldsymbol{C_1' = 18}$ pF $\boldsymbol{C_2 = 10}$ pF $\boldsymbol{C_r = 15}$ pF	$\boldsymbol{C_1' = 23}$ pF $\boldsymbol{C_2 = 10}$ pF $\boldsymbol{C_r = 12}$ pF	$\boldsymbol{C_1' = 35}$ pF $\boldsymbol{C_2 = 18}$ pF $\boldsymbol{C_r = 12}$ pF	$\boldsymbol{C_1' = 41}$ pF $\boldsymbol{C_2 = 18}$ pF $\boldsymbol{C_r = 12}$ pF	$\boldsymbol{C_1' = 48}$ pF $\boldsymbol{C_2 = 22}$ pF $\boldsymbol{C_r = 12}$ pF
151	4.2	9.5	9.6	9.7	9.7
182	3.3	8.3	8.7	8.9	8.7
268	1.7	6.2	6.9	7.1	7.0
329	0.7	4.9	5.7	5.8	5.8
400	-0.4	3.6	4.5	4.6	4.6

Table G.3: Spectrum analyzer input power against $R_{ex.}$ for C_1' = 55, 59, 64, 70 and 76 pF, $x = 2.0 \pm 0.3$.

$R_{ex.}(\Omega)$	$P_{S.A}$ (dBm)				
	$C_1' = 55$ pF $C_2 = 27$ pF $C_r = 12$ pF	$C_1' = 59$ pF $C_2 = 27$ pF $C_r = 12$ pF	$C_1' = 64$ pF $C_2 = 33$ pF $C_r = 12$ pF	$C_1' = 70$ pF $C_2 = 33$ pF $C_r = 12$ pF	$C_1' = 76$ pF $C_2 = 33$ pF $C_r = 12$ pF
0	14.7	14.5	15.3	15.4	15.5
6	14.5	14.3	15.2	15.3	15.4
10	14.4	14.1	15.0	15.1	15.2
15	14.3	14.0	14.9	14.9	15.0
22	14.0	13.7	14.3	14.7	14.8
39	13.4	13.1	14.1	14.0	14.2
47	13.2	13.0	13.9	13.7	14.0
56	12.8	12.5	13.5	13.4	13.6
68	12.6	12.3	13.2	13.0	13.3
75	12.4	12.2	13.1	12.8	13.1
82	12.2	11.6	12.9	12.5	12.9
99	11.6	11.4	12.3	12.0	12.3
120	11.0	10.8	11.6	11.3	11.6
127	10.8	10.7	11.5	11.0	11.5
151	9.9	10.1	10.7	10.4	10.9
182	8.6	9.2	9.9	9.3	10.0
268	7.5	7.4	7.9	None	7.9
329	6.3	6.2	6.6	None	6.6
400	5.0	4.9	5.2	None	5.2

Table G.4: Spectrum analyzer power against $R_{ex.}$ for $C_1' = 88$, 103, 109, and 128 pF, $x = 2.0 \pm 0.3$.

$\boldsymbol{R_{ex.}(\Omega)}$	$\boldsymbol{P_{S.A}}$ (dBm)			
	$\boldsymbol{C_1' = 88}$ pF $\boldsymbol{C_2 = 47}$ pF $\boldsymbol{C_r = 10}$ pF	$\boldsymbol{C_1' = 103}$ pF $\boldsymbol{C_2 = 56}$ pF $\boldsymbol{C_r = 10}$ pF	$\boldsymbol{C_1' = 109}$ pF $\boldsymbol{C_2 = 56}$ pF $\boldsymbol{C_r = 10}$ pF	$\boldsymbol{C_1' = 128}$ pF $\boldsymbol{C_2 = 68}$ pF $\boldsymbol{C_r = 10}$ pF
0	15.6	14.6	14.6	14.4
6	15.3	14.4	14.5	14.3
10	15.1	14.4	14.4	14.1
15	14.9	14.2	14.3	14.0
22	14.7	14.0	14.0	13.8
39	14.0	13.5	13.5	13.3
47	13.8	13.1	13.3	12.9
56	13.2	12.8	13.0	12.6
68	13.2	12.6	12.7	12.3
75	12.9	12.3	12.3	12.0
82	12.7	12.1	12.1	11.7
99	12.1	11.4	11.5	10.8
120	11.5	10.8	10.9	10.1
127	11.3	10.4	10.6	9.2
151	10.6	9.6	None	8.6
182	9.6	8.4	8.5	None
268	7.4	None	None	None
329	6.0	None	None	None
400	None	None	None	None